Nuclear Optical Potential

and associated tools

G. Blanchon

CEA,DAM,DIF F-91297 Arpajon, France

A journey into nuclear structure and reaction theory, Doctoral School Pheniics 2023

Outline

Outline

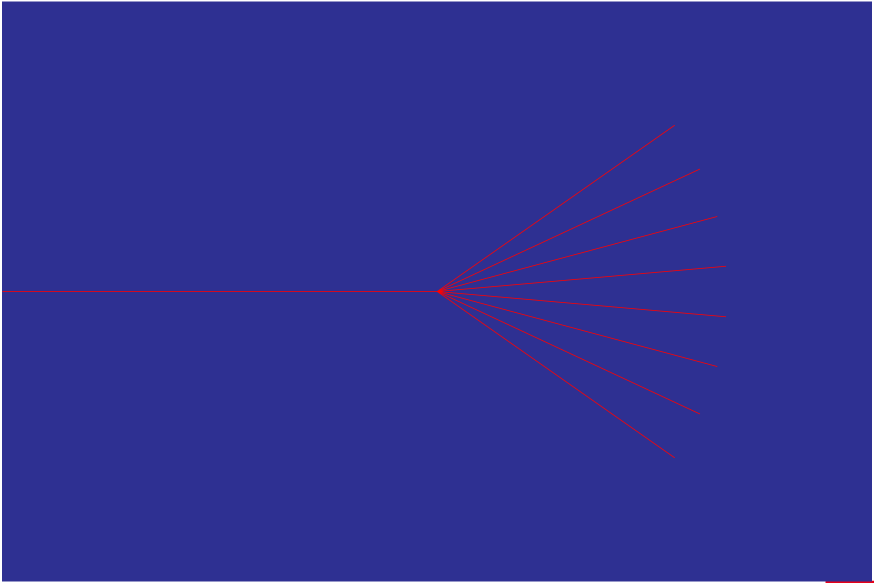

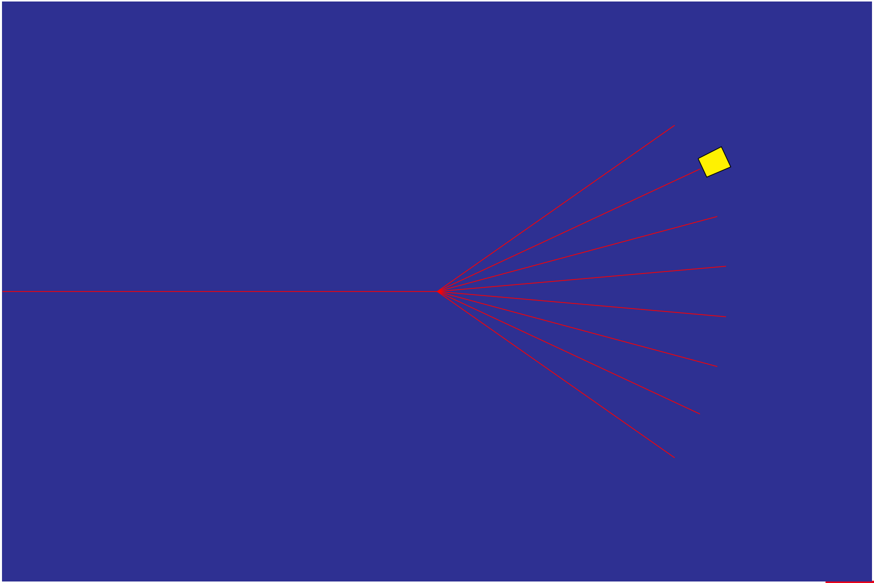

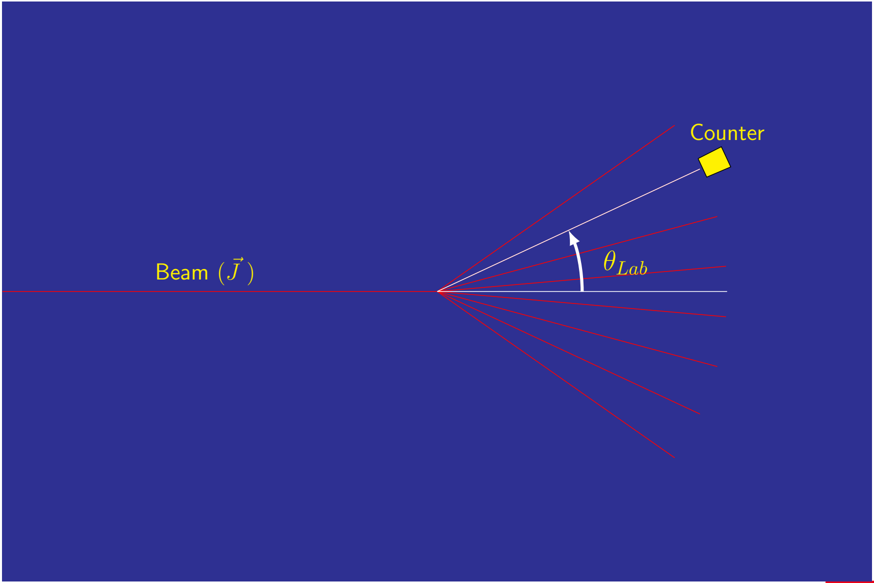
Counter
θ_{Lab}
Beam $(\vec{J})$

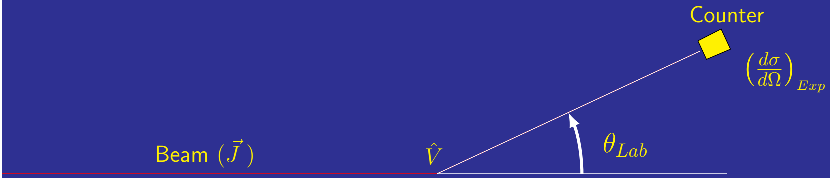

$$(\hat{K} + \hat{V})|\Psi\rangle = E|\Psi\rangle$$

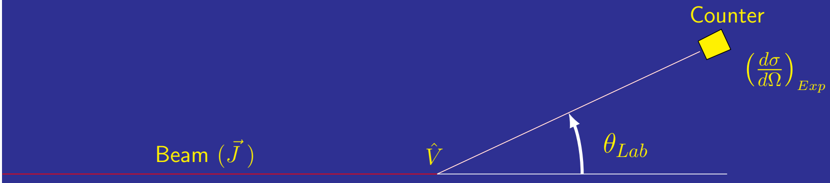

$$(\hat{K}+\hat{V})|\Psi\rangle = E|\Psi\rangle$$

Assuming $\hat{V}$ local: $\langle\vec{r}\,'|\hat{V}|\vec{r}\rangle = v(\vec{r})\,\delta(\vec{r}\,'-\vec{r})$

Then: $-\frac{\hbar^2}{2m}\nabla^2\Psi(\vec{r}) + v(\vec{r})\,\Psi(\vec{r}) = E\Psi(\vec{r})$

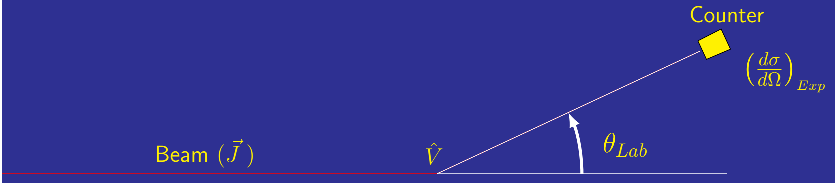

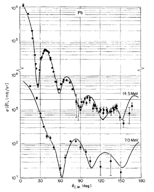

$$(\hat{K} + \hat{V})|\Psi\rangle = E|\Psi\rangle$$

Assuming $\hat{V}$ local: $\langle \vec{r}\,'|\hat{V}|\vec{r}\rangle = v(\vec{r})\,\delta(\vec{r}\,' - \vec{r})$

Then: $-\frac{\hbar^2}{2m}\nabla^2\Psi(\vec{r}) + v(\vec{r})\,\Psi(\vec{r}) = E\Psi(\vec{r}) \longrightarrow \left(\frac{d\sigma}{d\Omega}\right)_{Th}$

Challenges

We consider nucleon scattering off a target nucleus

- This is a $(A+1)$-body problem.
- Involving continuum, one can solve the few-body problem exactly.
  Here we are dealing with a many-body problem.
  For example Koning-Delaroche global potential is intended for A ranging from 24 to 209

(A. Koning and J.P. Delaroche, NPA 713, 231 (2003))

Challenges

We consider nucleon scattering off a target nucleus

- This is a $(A+1)$-body problem.
- Involving continuum, one can solve the few-body problem exactly.
  Here we are dealing with a many-body problem.
  For example Koning-Delaroche global potential is intended for A ranging from 24 to 209

(A. Koning and J.P. Delaroche, NPA 713, 231 (2003))

Feshbach talking about Weisskopf

"His was an unquenchable desire to understand the essential physical elements involved in a phenomenon to strip away the complexities of a detailed explaination and to make visible the underlying ideas and concepts."

(LNS 1992 Symposium https://www.youtube.com/watch?v=6I06GvMBvAE)

We consider nucleon scattering off a target nucleus

- This is a $(A + 1)$-body problem.
- Involving continuum, one can solve the few-body problem exactly.
  Here we are dealing with a many-body problem.
  For example Koning-Delaroche global potential is intended for A ranging from 24 to 209

(A. Koning and J.P. Delaroche, NPA 713, 231 (2003))

Feshbach talking about Weisskopf

"His was an unquenchable desire to understand the essential physical elements involved in a phenomenon to strip away the complexities of a detailed explaination and to make visible the underlying ideas and concepts."

(LNS 1992 Symposium https://www.youtube.com/watch?v=6I06GvMBvAE)

Main ideas

- Go from a $(A + 1)$-body to a 2-body problem made of a target and a projectile.
- Feed phenomenology with the main degrees of freedom obtained from microscopy

We consider nucleon scattering off a target nucleus

- This is a $(A+1)$-body problem.
- Involving continuum, one can solve the few-body problem exactly.
  Here we are dealing with a many-body problem.
  For example Koning-Delaroche global potential is intended for A ranging from 24 to 209

(A. Koning and J.P. Delaroche, NPA 713, 231 (2003))

Feshbach talking about Weisskopf

"His was an unquenchable desire to understand the essential physical elements involved in a phenomenon to strip away the complexities of a detailed explaination and to make visible the underlying ideas and concepts."

(LNS 1992 Symposium https : //www.youtube.com/watch?v = 6I06GvMBvAE)

Main ideas

- Go from a $(A+1)$-body to a 2-body problem made of a target and a projectile.
- Feed phenomenology with the main degrees of freedom obtained from microscopy

$\rightarrow$ Cloudy crystal ball model

(Feshbach, Porter, Weisskopf, Phys. Rev. 96, 448 (1954))

Challenges

We consider nucleon scattering off a target nucleus

- This is a $(A+1)$-body problem.
- Involving continuum, one can solve the few-body problem exactly.
  Here we are dealing with a many-body problem.
  For example Koning-Delaroche global potential is intended for A ranging from 24 to 209

(A. Koning and J.P. Delaroche, NPA 713, 231 (2003))

Feshbach talking about Weisskopf

"His was an unquenchable desire to understand the essential physical elements involved in a phenomenon to strip away the complexities of a detailed explaination and to make visible the underlying ideas and concepts."

(LNS 1992 Symposium https://www.youtube.com/watch?v=6I06GvMBvAE)

Main ideas

- Go from a $(A+1)$-body to a 2-body problem made of a target and a projectile.
- Feed phenomenology with the main degrees of freedom obtained from microscopy

$\rightarrow$ Optical Potential

(Feshbach, Porter, Weisskopf, Phys. Rev. 96, 448 (1954))

PHYSICAL REVIEW VOLUME 96, NUMBER 2 OCTOBER 15, 1954

Model for Nuclear Reactions with Neutrons*

H. FESHBACH, C. E. PORTER,† AND V. F. WEISSKOPF
Department of Physics and Laboratory for Nuclear Science, Massachusetts Institute of Technology, Cambridge, Massachusetts

(Received June 28, 1954)

A simple model is proposed for the description of the scattering and the compound nucleus formation by nucleons impinging upon complex nuclei. It is shown that, by making appropriate averages over resonances, an average problem can be defined which is referred to as the "gross-structure" problem. Solution of this problem permits the calculation of the average total cross section, the cross section for the formation of the compound nucleus, and the part of the elastic-scattering cross section which does not involve formation of the compound nucleus. Unambiguous definitions are given for the latter cross sections.

The model describing these properties consists in replacing the nucleus by a one-body potential which acts upon the incident nucleon. This potential $V=V_0+iV_1$ is complex; the real part represents the average potential in the nucleus; the imaginary part causes an absorption which describes the formation of the compound nucleus. As a first approximation a potential is used whose real part V_0 is a rectangular potential well and whose imaginary part is a constant fraction of the real part $V_1=\zeta V_0$.

This model is used to reproduce the total cross sections for neutrons, the angular dependence of the elastic scattering, and the cross section for the formation of the compound nucleus. It is shown that the average properties of neutron resonances, in particular the ratio of the neutron width to the level spacing, are connected with the gross-structure problem and can be predicted by this model.

The observed neutron total cross sections can be very well reproduced in the energy region between zero and 3 Mev with a well depth of 42 Mev, a factor ζ of 0.03, and a nuclear radius of $R=1.45\times10^{-13}A^{\frac{1}{3}}$ cm. The angular dependence of the scattering cross section at 1 Mev is fairly well reproduced by the same model. The theoretical and experimental values for the ratios of neutron width to level distance at low energies and the reaction cross sections at 1 Mev do not agree too well but they show a qualitative similarity.

Feshbach, Porter, Weisskopf, Phys. Rev. 96, 448 (1954)

PHYSICAL REVIEW VOLUME 96, NUMBER 2 OCTOBER 15, 1954

Model for Nuclear Reactions with Neutrons*

H. FESHBACH, C. E. PORTER,† AND V. F. WEISSKOPF
Department of Physics and Laboratory for Nuclear Science, Massachusetts Institute of Technology, Cambridge, Massachusetts

(Received June 28, 1954)

A simple model is proposed for the description of the scattering and the compound nucleus formation by nucleons impinging upon complex nuclei. It is shown that, by making appropriate averages over resonances, an average problem can be defined which is referred to as the "gross-structure" problem. Solution of this problem permits the calculation of the average total cross section, the cross section for the formation of the compound nucleus, and the part of the elastic-scattering cross section which does not involve formation of the compound nucleus. Unambiguous definitions are given for the latter cross sections.

The model describing these properties consists in replacing the nucleus by a one-body potential which acts upon the incident nucleon. This potential $V=V_0+iV_1$ is complex; the real part represents the average potential in the nucleus; the imaginary part causes an absorption which describes the formation of the compound nucleus. As a first approximation a potential is used whose real part V_0 is a rectangular potential well and whose imaginary part is a constant fraction of the real part $V_1=\zeta V_0$.

This model is used to reproduce the total cross sections for neutrons, the angular dependence of the elastic scattering, and the cross section for the formation of the compound nucleus. It is shown that the average properties of neutron resonances, in particular the ratio of the neutron width to the level spacing, are connected with the gross-structure problem and can be predicted by this model.

The observed neutron total cross sections can be very well reproduced in the energy region between zero and 3 Mev with a well depth of 42 Mev, a factor ζ of 0.03, and a nuclear radius of $R=1.45\times10^{-13}A^{\frac{1}{3}}$ cm. The angular dependence of the scattering cross section at 1 Mev is fairly well reproduced by the same model. The theoretical and experimental values for the ratios of neutron width to level distance at low energies and the reaction cross sections at 1 Mev do not agree too well but they show a qualitative similarity.

"It is this gross-structure problem and not the actual rapidly varying cross sections which we intend to describe by means of a one-particle problem with the potential"

Everything starts from experimental results

(A. Koning and J.P. Delaroche, NPA 713, 231 (2003))

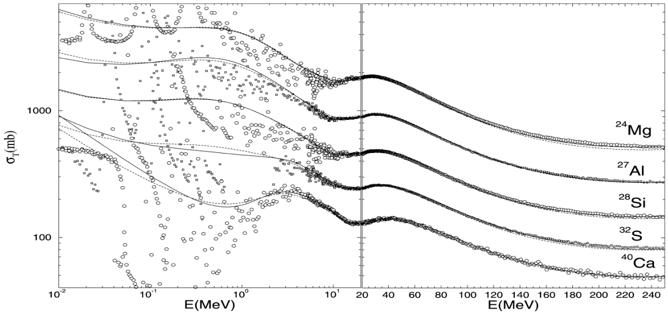

Fig. 2. Comparison of predicted neutron total cross sections and experimental data, for nuclides in the Mg–Ca mass region, for the energy range 10 keV–250 MeV. For more details, see Section 4.1.

Everything starts from experimental results

(A. Koning and J.P. Delaroche, NPA 713, 231 (2003))

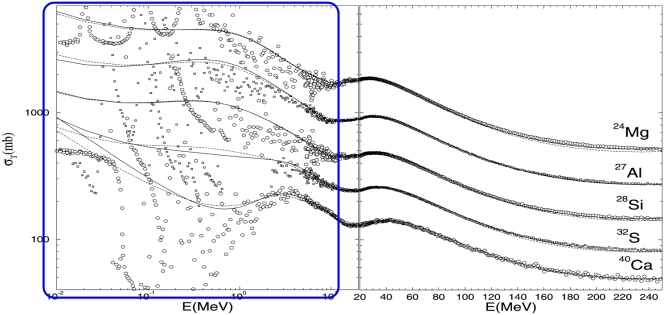

Fig. 2. Comparison of predicted neutron total cross sections and experimental data, for nuclides in the Mg–Ca mass region, for the energy range 10 keV–250 MeV. For more details, see Section 4.1.

Resonances region

Everything starts from experimental results

(A. Koning and J.P. Delaroche, NPA 713, 231 (2003))

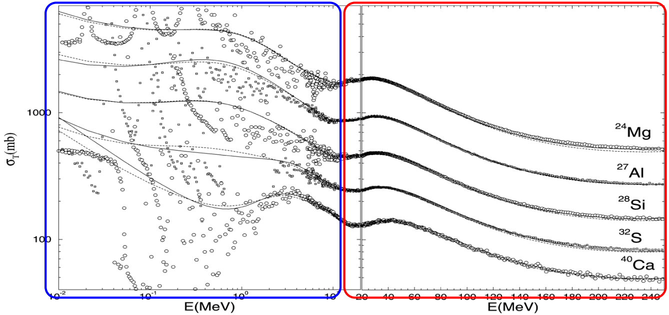

Fig. 2. Comparison of predicted neutron total cross sections and experimental data, for nuclides in the Mg–Ca mass region, for the energy range 10 keV–250 MeV. For more details, see Section 4.1.

Resonances region **Smooth region**

Everything starts from experimental results

n+^{209}Pu *(Figure from P. Tamagno)*

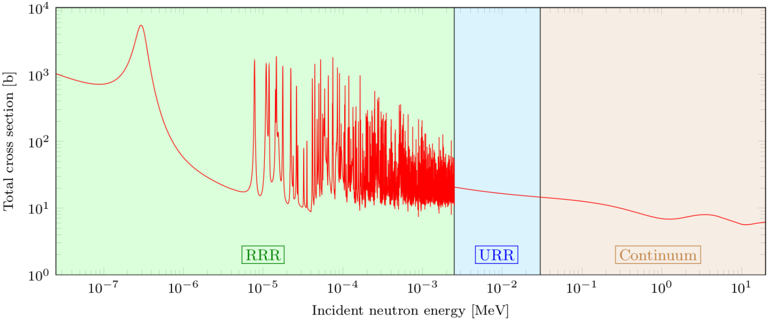

We consider Γ the width of the resonances and D the distance in energy between those resonances

- Resolved Resonance Regime: $D > \Gamma$
- Unresolved Resonance Regime: $D < \Gamma$
- Continuum

$$\tau \propto 1/\Gamma$$

Proton emission spectrum $p+{}^{54}Fe$ @ 61.7 MeV @ 60 deg.

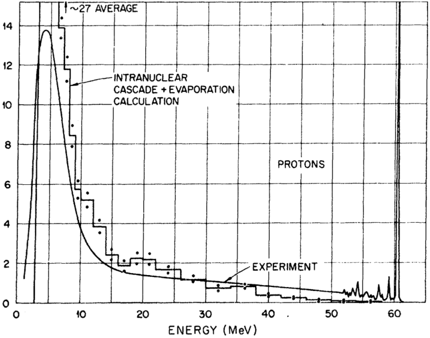

- Compound nucleus $\tau \approx 10^{-16}$s ("delayed")
- Pre-equilibriium
- Direct reaction $\tau \approx 10^{-22}$s ("prompt")

> *Nuclear reactions that occur in a* ***time comparable to the time of transit*** *of an incident particle across the nucleus (~10^{-22} s) are called* ***direct nuclear reactions.*** *Interaction time is critical for defining the reaction mechanism. The very short interaction time allows for an* ***interaction of a single nucleon*** *only (in extreme cases).*

The cross-sections for direct reactions vary smoothly and slowly with energy in contrast to the compound nucleus reactions. These cross-sections are comparable to the geometrical cross-sections of target nuclei. Types of direct reactions:

- **Elastic scattering** in which a passing particle and targes stay in their ground states.
- **Inelastic scattering** in which a passing particle changes its energy state. For example, the (p, p') reaction.
- **Transfer reactions** in which one or more nucleons are transferred to the other nucleus. These reactions are further classified as:
  - **Stripping reaction** in which one or more nucleons are transferred to a target nucleus from passing particles. For example, the neutron stripping in the (d, p) reaction.
  - **Pick-up reaction** in which one or more nucleons are transferred from a target nucleus to a passing particle. For example, the neutron pick-up in the (p, d) reaction.
- **Break-up reaction** in which a breakup of a projectile into two or more fragments occurs.
- **Knock-out reaction** in which a single nucleon or a light cluster is removed from the projectile by a collision with the target.

Direct Reactions vs. Compound Nucleus Reactions

Direct Reactions

- The direct reactions are fast and involve a **single-nucleon interaction**.
- The interaction time must be very short **(~10^{-22} s)**.
- The direct reactions require incident particle energy **larger than ~ 5 MeV/Ap**. (Ap is the atomic mass number of a projectile)
- Incident particles interact **on the surface** of a target nucleus rather than in the volume of a target nucleus.
- Products of the direct reactions **are not distributed isotropically in angle**, but they are forward-focused.
- Direct reactions are of importance in measurements of nuclear structure.

Compound Nucleus Reactions

- The compound nucleus reactions involve **many nucleon-nucleon interactions**.
- A large number of collisions between the nucleons leads to a **thermal equilibrium** inside the compound nucleus.
- The time scale of compound nucleus reactions is **10^{-18} s – 10^{-16} s**.
- The compound nucleus reactions are usually created if the projectile has **low energy**.
- Incident particles interact in the volume of a target nucleus.
- Products of the compound nucleus reactions are distributed **near isotropically in angle** (the nucleus loses memory of how it was created – ***Bohr's hypothesis of independence***).
- **The decay mode** of the compound nucleus **does not depend on how the compound nucleus is formed**.
- Resonances in the cross-section are typical for the compound nucleus reaction.

the separation of nuclear reaction mechanisms into direct and compound is too simplistic...

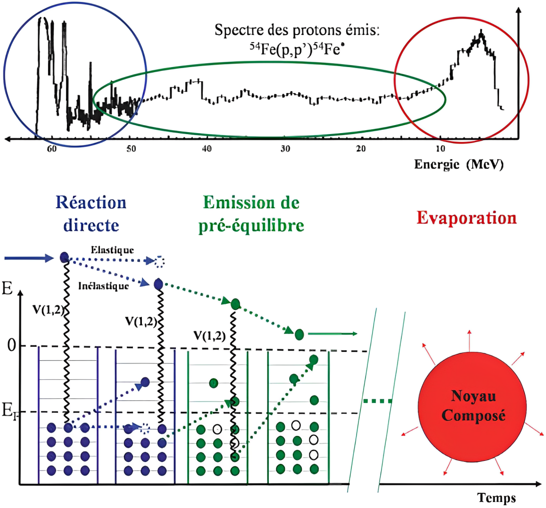

Many processes to describe: need for models and codes

... organized in a consistent way.

TALYS, CONRAD, EMPIRE...

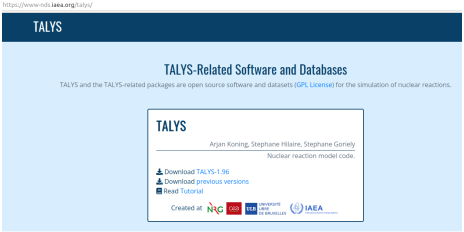

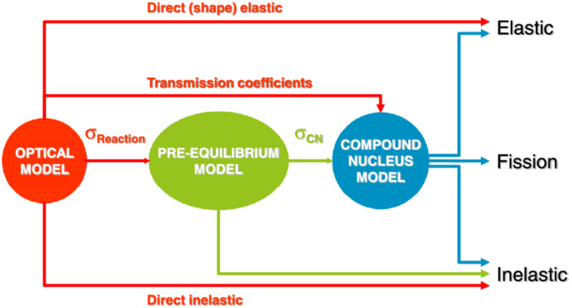

Philosophy of Talys: "First completeness then quality"

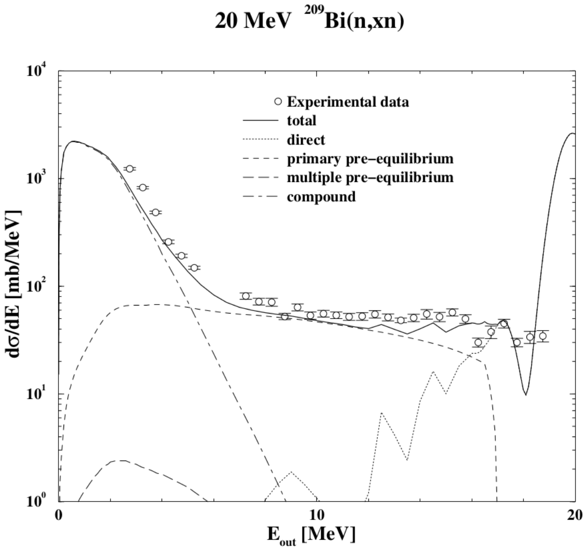

Figure 4.10: ^{209}Bi (n,xn) spectrum at 20 MeV. Experimental data are obtained from [9].

Outline

Averaging energy separates the prompt part of the reaction from the delayed part
$\rightarrow$ Optical potential describes the prompt contribution

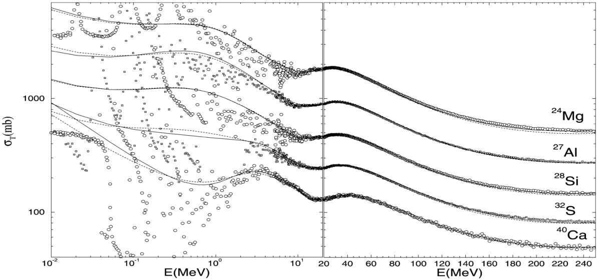

Fig. 2. Comparison of predicted neutron total cross sections and experimental data, for nuclides in the Mg–Ca mass region, for the energy range 10 keV–250 MeV. For more details, see Section 4.1.

(A. Koning and J.P. Delaroche, NPA 713, 231 (2003))

Challenges

Picture from C. Hebborn et al. J. Phys. G: Nucl. Part. Phys. 50 (2023) 060501

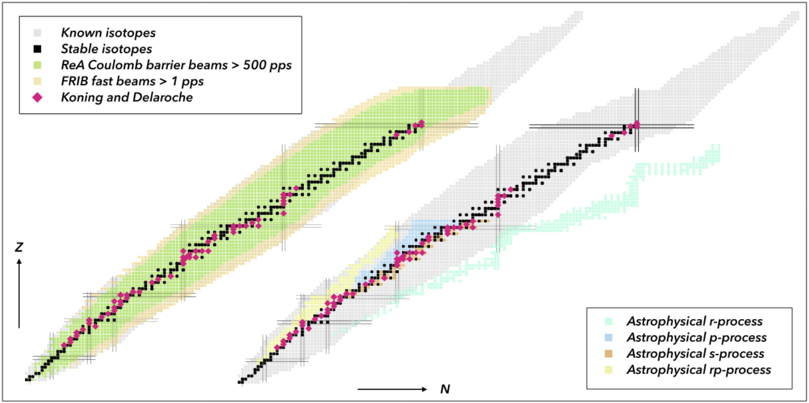

Picture from C. Hebborn et al. J. Phys. G: Nucl. Part. Phys. 50 (2023) 060501

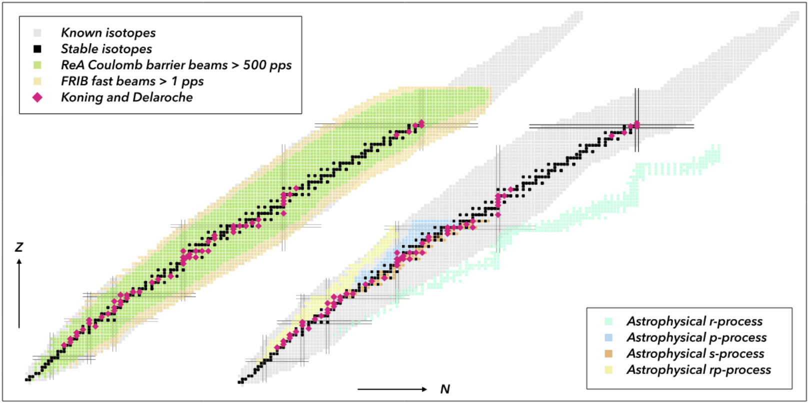

- Need for potentials valid for exotic nuclei
- Extrapolation driven by microscopy?

Outline

- Consider a beam of particles hitting a thin sheet of material
- $N_i = J_i S$ incident particles hit the surface per second
- N_c outgoing particles counted per second (only count particles belonging to an outgoing channel c. For instance elastic channel: detection of a particle with the same energy than the incident particle)
- Probability P_c of reaction: $P_c = \frac{N_c}{N_i} = \frac{N_c}{J_i S}$

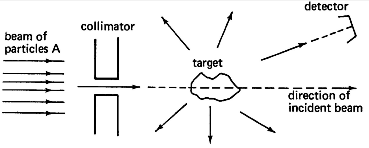

- The cross section σ_c is an effective area associated to one target nucleus, that provides a measure of the probability of reaction in the channel c.
- $\Sigma_c = \sigma_c N_t$ ($N_t = nSdx$ number of target nuclei) is the portion of the surface S which, when hit by the incident particle, will lead to the reaction channel c.

$$P_c = \frac{\Sigma_c}{S} = \frac{N_c}{J_i S}, \quad \sigma_c = \frac{N_c}{N_t}\frac{1}{J_i} = \frac{\text{reaction rate}}{\text{incident flux}}$$

Schrödinger equation with a spherical potential

$$
\begin{aligned}
H|\psi\rangle = (T+V)|\psi\rangle &= E|\psi\rangle \\
\int \langle \mathbf{r}|(T+V)|\mathbf{r}'\rangle\langle\mathbf{r}'|\psi\rangle d\mathbf{r}' &= E\langle\mathbf{r}|\psi\rangle
\end{aligned}
$$

Kinetic part

$$
\begin{aligned}
T &= \frac{\mathbf{P}^2}{2m} \\
\langle \mathbf{r}|\mathbf{P}^2|\mathbf{r}'\rangle &= \int \langle \mathbf{r}|\mathbf{P}^2|\mathbf{p}\rangle\langle\mathbf{p}|\mathbf{r}'\rangle d\mathbf{p} \\
&= \int \langle \mathbf{r}|\mathbf{p}\rangle\mathbf{p}^2\langle\mathbf{p}|\mathbf{r}'\rangle d\mathbf{p} \\
&= \frac{1}{(2\pi\hbar)^3}\int \mathbf{p}^2 e^{\frac{i}{\hbar}\mathbf{p}.(\mathbf{r}\text{-}\mathbf{r}')} d\mathbf{p} \\
&= -\hbar^2\delta''(\mathbf{r}\text{-}\mathbf{r}') \\
\langle \mathbf{r}|T|\psi\rangle &= -\frac{\hbar^2}{2m}\Delta\psi(\mathbf{r})
\end{aligned}
$$

Potential part

$$
\begin{aligned}
\langle \mathbf{r}|V|\psi\rangle &= \int d\mathbf{r}'\langle\mathbf{r}|V|\mathbf{r}'\rangle\langle\mathbf{r}'|\psi\rangle \\
\langle \mathbf{r}|V|\mathbf{r}'\rangle &\equiv V(\mathbf{r},\mathbf{r}')
\end{aligned}
$$

Local potential

$$V(\mathbf{r},\mathbf{r}') = V(r)\delta(\mathbf{r},\mathbf{r}')$$

Schrödinger equation with a spherical potential

$$-\frac{\hbar^2}{2m}\Delta\psi(\mathbf{r}) + \int d\mathbf{r}' V(\mathbf{r},\mathbf{r}')\psi(\mathbf{r}') = E\psi(\mathbf{r})$$

Spherical coordinates,

$$\left.\begin{aligned} \Delta \equiv & \quad p_r^2 + \frac{\mathbf{l}^2}{r^2} \\ p_r^2 = & \quad -\hbar^2 \frac{1}{r}\frac{d^2}{dr^2} r \end{aligned}\right\} \langle \mathbf{r}|T|\psi\rangle = \left[-\frac{\hbar^2}{2m}\frac{1}{r}\frac{d^2}{dr^2}r + \frac{\mathbf{l}^2}{2mr^2}\right]\psi(\mathbf{r})$$

Using the following multipole expansions and projecting on $|ljm\rangle$

$$\psi(\mathbf{r}) = \sum_{ljm} \frac{u_{jlm}(r)}{r}\mathcal{Y}_{jl}^m(\hat{\mathbf{r}}) \quad \text{and} \quad \nu_{ljm}(r,r') = \iint d\hat{\mathbf{r}} d\hat{\mathbf{r}}' \mathcal{Y}_{jl}^m(\hat{\mathbf{r}}) V(\mathbf{r},\mathbf{r}')\mathcal{Y}_{jl}^{m\dagger}(\hat{\mathbf{r}}')$$

Integro-differential Schrödinger equation

$$-\frac{\hbar^2}{2m}\left[\frac{d^2}{dr^2} - \frac{l(l+1)}{r^2}\right]u_{ljm}(r) + \int dr' r\nu_{ljm}(r,r')r' u_{jlm}(r') = E\ u_{ljm}(r)$$

Absorption by a complex potential

Probability current:

$$\mathbf{j(r)} = -i\frac{\hbar}{2\mu}\left(\phi^*(\mathbf{r})\nabla\phi(\mathbf{r}) - \phi(\mathbf{r})\nabla\phi^*(\mathbf{r})\right)$$

Schrödinger Equation:

$$\left(\frac{\hbar^2}{2\mu}\nabla^2 + (U(r) + iW(r))\right)\phi(\mathbf{r}) = E\phi(\mathbf{r})$$

$\phi^*(\mathbf{r}) \times \{S.E.\} - \phi(\mathbf{r})\,\{S.E.\}^*$:

Flux variation: $\nabla.\mathbf{j} = \dfrac{i}{\hbar}(V^*(r) - V(r))|\phi(r)|^2 = \dfrac{2}{\hbar}W(r)|\phi(r)|^2$

→ Negative imaginary potential: flux absorption
→ Positive imaginary potential: flux creation

Absorption by a complex potential

Probability current:

$$\mathbf{j(r)} = -i\frac{\hbar}{2\mu}\left(\phi^*(\mathbf{r})\nabla\phi(\mathbf{r}) - \phi(\mathbf{r})\nabla\phi^*(\mathbf{r})\right)$$

Schrödinger Equation:

$$\left(\frac{\hbar^2}{2\mu}\nabla^2 + (U(r) + iW(r))\right)\phi(\mathbf{r}) = E\phi(\mathbf{r})$$

$\phi^*(\mathbf{r}) \times \{S.E.\} - \phi(\mathbf{r})\,\{S.E.\}^*$:

$$\text{Flux variation: } \nabla.\mathbf{j} = \frac{i}{\hbar}(V^*(r) - V(r))|\phi(r)|^2 = \frac{2}{\hbar}W(r)|\phi(r)|^2$$

→ **Negative imaginary potential: flux absorption**
→ ~~**Positive imaginary potential: flux creation**~~

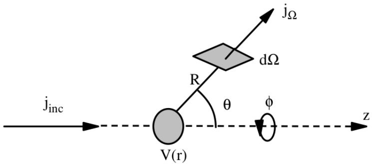

At $r \to \infty$, the incident wave function is a plane wave $\chi_{inc}(\mathbf{r}) = \exp(i\mathbf{k}.\mathbf{r})$ and the scattered wave is spherical $\chi_{el}(\mathbf{r}) = f(\Omega)\frac{\exp(ikr)}{r}$.
The complete wave function reads

$$\chi(\mathbf{r} \to \infty) = \exp(i\mathbf{k}.\mathbf{r}) + f(\Omega)\frac{\exp(ikr)}{r}$$

where f is the scattering amplitude and χ is the solution of the Schrödinger equation

$$(H - E)\chi = 0$$

Elastic cross section

We want to determine $d\sigma_{el}(\Omega)$ the element of elastic cross section in the direction Ω. It reads

$$d\sigma_{el}(\Omega) = \frac{\mathbf{j}_{el}(\Omega)}{\mathbf{j}_{inc}},$$

with $\mathbf{j}_{el}(\Omega)$ the exit flux in the direction Ω and $\mathbf{j}_{inc}$ the incident flux

$$\mathbf{j}_{inc} = \frac{\hbar}{\mu}\mathbf{k}.$$

the scattered flux in the direction Ω through the solid angle $d\Omega$ is

$$\mathbf{j}_{el}(\Omega) r^2 d\Omega = \frac{\hbar}{2i\mu}\left[f^*(\Omega)\frac{\exp(-ikr)}{r}\frac{d}{dr}\left(f(\Omega)\frac{\exp(ikr)}{r}\right) - f(\Omega)\frac{\exp(ikr)}{r}\frac{d}{dr}\left(f^*(\Omega)\frac{\exp(-ikr)}{r}\right)\right]$$

Developing and simplifying, we get

$$\mathbf{j}_{el}(\Omega) r^2 d\Omega = |f(\Omega)|^2 \frac{\hbar}{\mu} k d\Omega$$

and finally, we get the expression for the differential cross section

$$\frac{d\sigma_{el}}{d\Omega} = |f(\Omega)|^2$$

Partial-wave expansion

All the information about scattering is contained into $f(\Omega)$

Let's now consider the partial wave exapansion of the Schrödinger equation:

$$\boxed{\left(\frac{d^2}{dr^2} - \frac{l(l+1}{r^2} - \frac{2\mu}{\hbar^2}V(r) + k^2\right) u_l(r) = 0}$$

$$k^2 = \frac{2\mu E}{\hbar^2}.$$

and

$$\chi(\vec{r}) = \frac{1}{kr}\sum_{l=0}^{\infty}(2l+1)\ i^l\ u_l(r)\ P_l(\cos(\theta)),$$

Taking the limit $r \to \infty$

$$\left(\frac{d^2}{dr^2} + k^2\right) u_l(r \to \infty) = 0.$$

$$u_l(r \to \infty) = a_l \frac{i^{-l}e^{i\delta_l}e^{ikr} - i^l e^{-i\delta_l}e^{-ikr}}{2i}$$

with δ_l the phaseshift. The effect of the potential is shift the asymptotic part of the wave function.

Partial-wave expansion

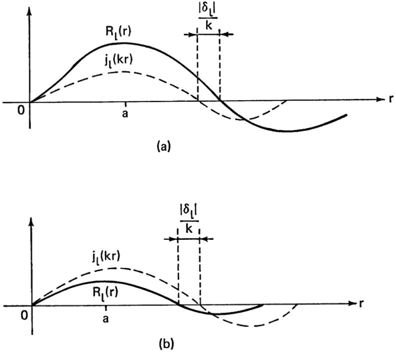

Schematic representation of the effect on the free radial wave $j_l(kr)$ of (a) a repulsive (positive) potential, (b) an attractive (negative) potential.

The phaseshift is energy dependent, real if the potential is real, complex if the potential is complex. In the spherical case, it is diagonal in (l,j) with j=l+s.

(Picture from C. Joachain)

Partial-wave expansion

We proceed now to the partial-wave expansion of the solution

$$\chi(\vec{r}) = \frac{1}{2ik}\sum_{l=0}^{\infty}(2l+1)\ P_l(\cos(\theta))\left((-)^{l+1}\frac{e^{-ikr}}{r} + (1+2\ i\ k\ f_l)\frac{e^{ikr}}{r}\right).$$

using the partial-wave expansion of the plane wave

$$e^{i\vec{k}.\vec{r}} = e^{ik\ r\ \ \cos(\theta)} = \sum_{l=0}^{\infty}(2l+1)\ i^l\ j_l(kr)\ P_l(\cos\theta)$$

The expansion of the solution can also be obtained using

$$\chi(\vec{r}) = \frac{1}{kr}\sum_{l=0}^{\infty}(2l+1)\ i^l\ u_l(r)\ P_l(\cos(\theta)),$$

and

$$u_l(r\to\infty) = a_l\frac{i^{-l}e^{i\delta_l}e^{ikr} - i^l e^{-i\delta_l}e^{-ikr}}{2i}$$

then

$$\chi(\vec{r}) = \frac{1}{2ik}\sum_{l=0}^{\infty}(2l+1)\ P_l(\cos(\theta))a_l\left((-)^{l+1}e^{-i\delta_l}\frac{e^{-ikr}}{r} + e^{i\delta_l}\frac{e^{ikr}}{r}\right).$$

Partial-wave expansion

By identification of the two solutions, we get

$$1 = a_l e^{-i\delta_l}$$

and

$$(1 \ + \ 2 \ i \ k \ f_l) \ = \ a_l e^{i\delta_l}$$

Finally we get an expression for the partial-wave expansion of the scattering amplitude

$$\boxed{f_l = \frac{1}{2ik}\left(e^{2i\delta_l} - 1\right)}$$

where $S_l = \exp(2i\delta_l)$ is called S-matrix or scattering matrix.
Thus

$$f(\theta) = \frac{1}{2ik}\sum_{l=0}^{\infty}(2l+1)(S_l - 1)P_l(\cos\theta)$$

Then we have the cross section

$$\frac{d\sigma_{el}}{d\Omega} \quad = \quad |f(\theta)|^2 \qquad (1)$$

We finally get the expression for the **differential cross section**

$$\frac{d\sigma_{el}}{d\Omega} \quad = \quad \frac{1}{4k^2}\sum_{l,l'=0}^{\infty}(2l+1)(2l'+1)(S_l - 1)(S_{l'}^* - 1)P_l(\cos\theta)P_{l'}(\cos\theta)$$

Example of differential cross section

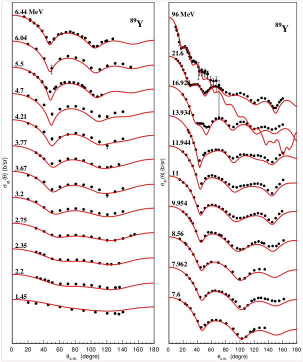

$$\boxed{\frac{d\sigma_{el}}{d\Omega} = |f(\theta)|^2 = \frac{1}{4k^2}\sum_{l,l'=0}^{\infty}(2l+1)(2l'+1)(S_l-1)(S_{l'}^*-1)P_l(\cos(\theta))P_{l'}(\cos(\theta))}$$

Integral cross sections

One can get the integral cross section by integrating the differential cross section on the angle

$$\sigma_{el} = \int_{-1}^{1} \frac{d\sigma_{el}}{d\Omega} d(\cos\theta)$$

$$\sigma_{el} = \frac{\pi}{k^2} \sum_{l=0}^{\infty} |S_l - 1|^2$$

Integral cross sections

(zero-spin projectile and target)

Shape Elastic cross section

$$\sigma_{SE} = \frac{\pi}{k^2} \sum_{\ell} |1 - S_\ell|^2$$

Inelastic cross section

$$\sigma_{Inel} = \frac{\pi}{k^2} \sum_{\ell} 1 - |S_\ell|^2$$

Total cross section

$$\sigma_{T} = \frac{\pi}{k^2} \sum_{\ell} 1 - \mathrm{Re}(S_\ell)$$

with $S_\ell = e^{i2\delta_\ell}$.

Total Elastic Reaction

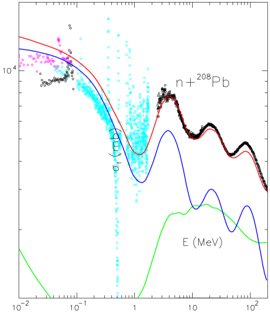

FIG. 4 – Sections efficaces Totale (rose), Elastique (bleu) et de Réaction (vert) d'un neutron sur du ^{208}Pb entre 10 keV et 200 MeV.

Example of integral cross section

Total Elastic Reaction

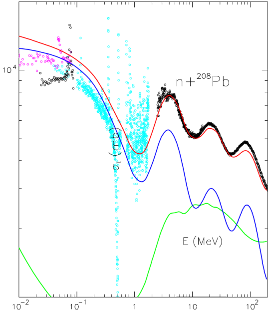

FIG. 4 – Sections efficaces Totale (rose), Elastique (bleu) et de Réaction (vert) d'un neutron sur du ^{208}Pb entre 10 keV et 200 MeV.

We know how to relate the cross section to phaseshift.
Now we need to determine the phaseshift

Matching with asymptotic form...

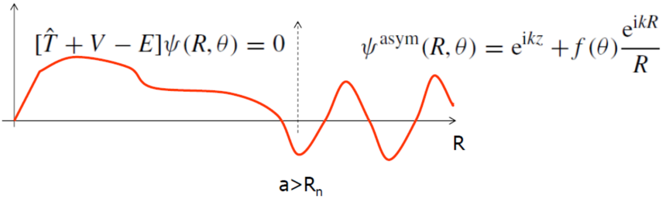

R_n : some large R where $V(R) \approx 0$ (potential dependent)

(Picture from C. Elster)

Matching with asymptotic form...

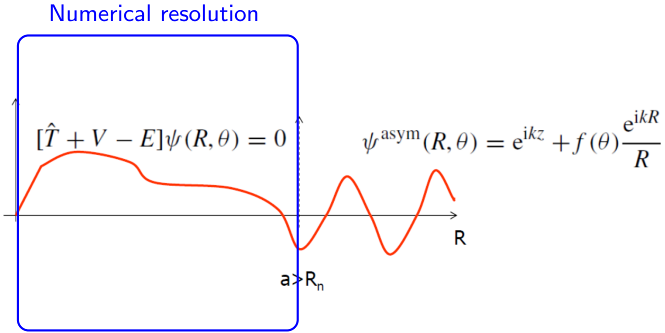

R_n : some large R where $V(R) \approx 0$ (potential dependent)

(Picture from C. Elster)

Matching with asymptotic form...

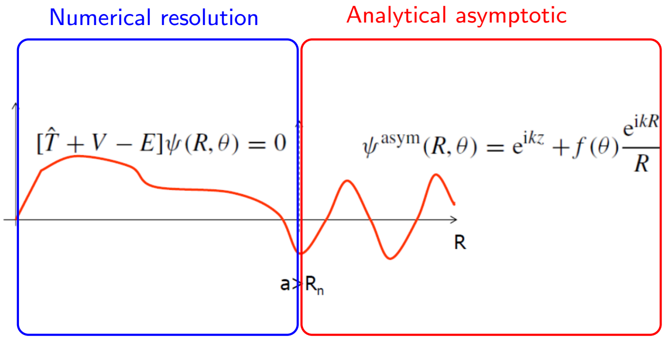

R_n : some large R where $V(R) \approx 0$ (potential dependent)

...Gives you access to phaseshift

(Further in the talk, we'll see how it works numerically)

(Picture from C. Elster)

Going back to energy averaging...

$$S = \langle S \rangle + \widehat{S}$$

Averaged cross section

$$\begin{aligned}
\langle \sigma_E \rangle &= \frac{\pi}{k^2} \langle |1 - S|^2 \rangle \\
\langle \sigma_R \rangle &= \frac{\pi}{k^2} \langle 1 - |S|^2 \rangle \\
\langle \sigma_T \rangle &= \frac{\pi}{k^2} \langle 1 - Re[S] \rangle
\end{aligned}$$

Averaged potential

$$\begin{aligned}
\bar{\sigma_E} &= \frac{\pi}{k^2} |1 - \langle S \rangle|^2 \\
\bar{\sigma_R} &= \frac{\pi}{k^2} (1 - |\langle S \rangle|^2) \\
\bar{\sigma_T} &= \frac{\pi}{k^2} (1 - Re[\langle S \rangle])
\end{aligned}$$

$$\begin{aligned}
\langle \sigma_E \rangle &= \bar{\sigma_E} + \sigma_{CE} \\
\langle \sigma_R \rangle &= \bar{\sigma_R} - \sigma_{CE} \\
\langle \sigma_T \rangle &= \bar{\sigma_T}
\end{aligned}$$

Compound elastic

$$\sigma_{CE} = \frac{\pi}{k^2} \langle |\widehat{S}|^2 \rangle$$

- TALYS: Hauser-Feshbach/ Koning-Delaroche
- particularly relevant for neutron scattering below 10 MeV

In the case of deformed rotating or/and vibrating targets...

$$(T_\alpha - \langle\alpha|V|\alpha\rangle + \epsilon_\alpha - E)u_\alpha(\mathbf{r}_\alpha) \quad = \quad -\sum_{\alpha'\neq\alpha}\langle\alpha|V|\alpha'\rangle u_{\alpha'}(\mathbf{r}_\alpha)$$

- Generalized optical potential
- Phaseshift is not diagonal anymore

Framework

$$\left(\hat{H}_{PP} + \hat{H}_{PQ}\frac{1}{E - \hat{H}_{QQ} + i\varepsilon}\hat{H}_{QP}\right)|\Psi\rangle = EP|\Psi\rangle$$

$$P|\Psi\rangle = \sum_{i=0}^{N} |\psi_i\rangle \oplus |w_i\rangle$$

$$P\hat{V}_{\text{Eff.}}P$$

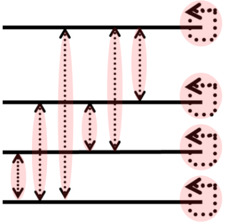

$$\begin{cases} \left(E - \hat{T} - \langle\psi_0|\hat{V}_{\text{Eff.}}|\psi_0\rangle\right)|w_0\rangle = \sum_{i\neq 0}\langle\psi_0|\hat{V}_{\text{Eff.}}|\psi_i\rangle|w_i\rangle \\ \left(E' - \hat{T} - \langle\psi_N|\hat{V}_{\text{Eff.}}|\psi_N\rangle\right)|w_N\rangle = \sum_{i\neq N}\langle\psi_N|\hat{V}_{\text{Eff.}}|\psi_i\rangle|w_i\rangle \end{cases}$$

One-body potentials

(Full)-Folding, **Local Density Approximation** (LDA).

Two-body interaction : one-body density matrix, radial densities.

5

Slide from M. Dupuis

Outline

Definitions

The state $|\alpha, t_0\rangle$ of a particle with quantum numbers α at time t_0 evolves in

$$|\alpha, t_0; t\rangle = e^{-\frac{i}{\hbar}H(t-t_0)}|\alpha, t_0\rangle$$

at a time t ($t > t_0$) and for a time-independent Hamiltonian.

$$\begin{aligned}
\psi(\mathbf{r}, t) &= \langle \mathbf{r}|\alpha, t_0; t\rangle = \langle \mathbf{r}|e^{-\frac{i}{\hbar}H(t-t_0)}|\alpha, t_0\rangle \\
&= \int d\mathbf{r'} \langle \mathbf{r}|e^{-\frac{i}{\hbar}H(t-t_0)}|\mathbf{r'}\rangle\langle \mathbf{r'}|\alpha, t_0\rangle \\
&= i\hbar \int d\mathbf{r'}\, G(\mathbf{r}, \mathbf{r'}; t - t_0)\psi(\mathbf{r'}, t_0)
\end{aligned}$$

where G is referred to as

Propagator or Green's Function

$$G(\mathbf{r}, \mathbf{r'}; t - t_0) = -\frac{i}{\hbar}\langle \mathbf{r}|e^{-\frac{i}{\hbar}H(t-t_0)}|\mathbf{r'}\rangle$$

Propagator or Green's Function

$$G(\mathbf{r}, \mathbf{r'}; t - t_0) = -\frac{i}{\hbar} \langle \mathbf{r} | e^{-\frac{i}{\hbar} H(t-t_0)} | \mathbf{r'} \rangle$$

$$\psi(\mathbf{r}, t) = i\hbar \int d\mathbf{r'} G(\mathbf{r}, \mathbf{r'}; t - t_0) \psi(\mathbf{r'}, t_0)$$

The wave function at **r** and t is determined by the wave function at the original time t_0, receiving contributions from all **r'** weighted by the amplitude G.

Operators and Statistics

Second quantization

$\psi^\dagger(\mathbf{r}, t)$ creates a particle at $(\mathbf{r}, t)$
$\psi(\mathbf{r}, t)$ annihilates a particle at $(\mathbf{r}, t)$

Bose-Einstein statistics (-)/Fermi-Dirac statistics (+)

$$\begin{aligned}
\left[\psi^\dagger(\mathbf{r}, t), \psi^\dagger(\mathbf{r'}, t)\right]_\pm &= 0 \\
\left[\psi(\mathbf{r}, t), \psi(\mathbf{r'}, t)\right]_\pm &= 0 \\
\left[\psi(\mathbf{r}, t), \psi^\dagger(\mathbf{r'}, t)\right]_\pm &= \delta(\mathbf{r} - \mathbf{r'})
\end{aligned}$$

$$
\begin{aligned}
G(\mathbf{r},\mathbf{r'};t-t_0) &= -\frac{i}{\hbar}\langle\mathbf{r}|e^{-\frac{i}{\hbar}H(t-t_0)}|\mathbf{r'}\rangle = -\frac{i}{\hbar}\langle 0|a_{\mathbf{r}}e^{-\frac{i}{\hbar}H(t-t_0)}a^{\dagger}_{\mathbf{r'}}|0\rangle \\
&= -\frac{i}{\hbar}\sum_{nn'}\langle 0|a_{\mathbf{r}}|n\rangle\langle n|e^{-\frac{i}{\hbar}H(t-t_0)}|n'\rangle\langle n'|a^{\dagger}_{\mathbf{r'}}|0\rangle
\end{aligned}
$$

One-body propagator in second quantization

$$G(1,1') = -i\langle 0|\mathcal{T}(\psi(1)\psi^{\dagger}(1'))|0\rangle$$

$\mathcal{T}$ is the time ordering operator and $1 \equiv \mathbf{r}_1, t_1$

$$
\begin{aligned}
\text{Ex: } \mathcal{T}(\psi(1)\psi^{\dagger}(1')) &= \psi(1)\psi^{\dagger}(1') \quad \text{if } t_1 > t_{1'} \\
&= -\psi^{\dagger}(1')\psi(1) \quad \text{if } t_1 < t_{1'}
\end{aligned}
$$

$$G(\mathbf{r},\mathbf{r'};t-t_0) = -\frac{i}{\hbar}\langle\mathbf{r}|e^{-\frac{i}{\hbar}H(t-t_0)}|\mathbf{r'}\rangle = -\frac{i}{\hbar}\langle 0|a_{\mathbf{r}}e^{-\frac{i}{\hbar}H(t-t_0)}a^\dagger_{\mathbf{r'}}|0\rangle$$
$$= -\frac{i}{\hbar}\sum_{nn'}\langle 0|a_{\mathbf{r}}|n\rangle\langle n|e^{-\frac{i}{\hbar}H(t-t_0)}|n'\rangle\langle n'|a^\dagger_{\mathbf{r'}}|0\rangle$$

One-body propagator in second quantization

$$G(1,1') = -i\langle 0|\mathcal{T}(\psi(1)\psi^\dagger(1'))|0\rangle$$

$\mathcal{T}$ is the time ordering operator and $1 \equiv \mathbf{r}_1, t_1$

Particle propagator $t_1 > t_{1'}$

$$G_1(1,1') = i\langle 0|\psi(1)\psi^\dagger(1')|0\rangle$$

Hole propagator $t_1 < t_{1'}$

$$G_1(1,1') = -i\langle 0|\psi^\dagger(1')\psi(1)|0\rangle$$

Gut feeling: it should be related to scattering...

n-body Green's function

$$G_n = (-i)^n \langle 0 | \mathcal{T}\{\psi(1)...\psi(n)\psi^\dagger(n')...\psi^\dagger(1')\} | 0 \rangle$$

Green's functions are average value
of
creation and annihilation operators

Road map

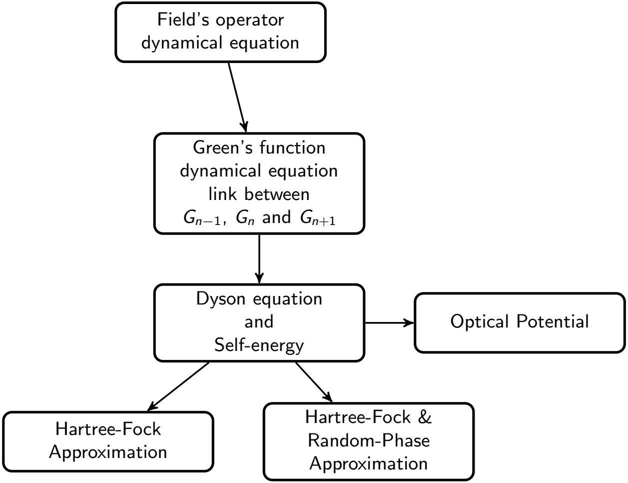

Field's operator dynamical equation
Green's function dynamical equation link between G_{n-1}, G_n and G_{n+1}
Dyson equation and Self-energy
Optical Potential
Hartree-Fock Approximation
Hartree-Fock & Random-Phase Approximation

Road map

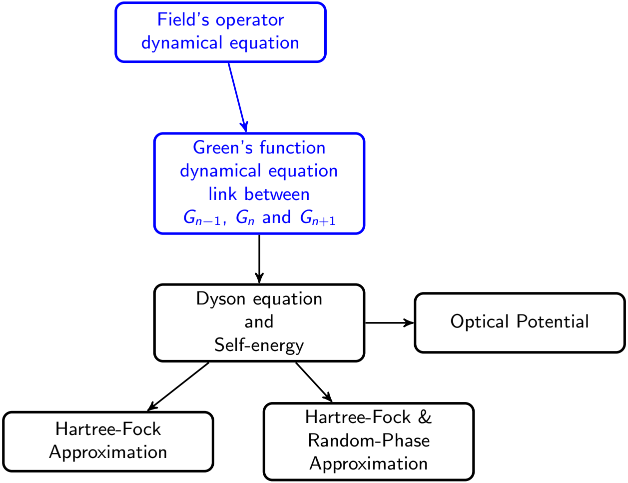

You will find the demonstration at the end of presentation

Dynamical equation for G_1

$$G_1(1,1') = G_0(1,1') - i \int d2d3 G_0(1,2) v(2,3) G_2(23;1'3^+)$$

The dynamical equation for the one-body Green's function connects G_0, G_1 and G_2.

More generally, the same kind of relation relates G_{N-1}, G_N and G_{N+1}.

Road map

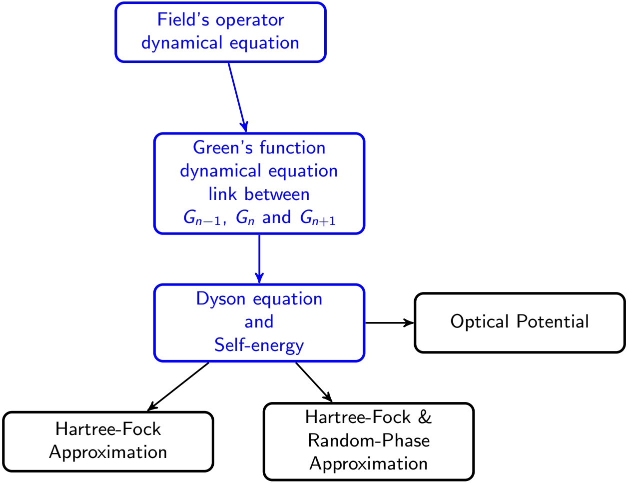

Field's operator dynamical equation
Green's function dynamical equation link between G_{n-1}, G_n and G_{n+1}
Dyson equation and Self-energy
Optical Potential
Hartree-Fock Approximation
Hartree-Fock & Random-Phase Approximation

Dyson equation

$$G_1(1,1') = G_0(1,1') + \int d2d3\, G_0(1,2) \underbrace{\Sigma(2,3)}_{\text{Self-energy}} G_1(3,1')$$

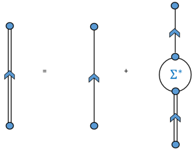

Figure 2.2: Graphical representation of the Dyson equation for the dressed SP propagator in terms of the noninteracting one and the irreducible self-energy.

Dynamical equation for G_1

$$G_1(1,1') = G_0(1,1') - i\int d2d3G_0(1,2)v(2,3)G_2(23;1'3^+)$$

Dyson equation

$$G_1(1,1') = G_0(1,1') + \int d2d3G_0(1,2)\underbrace{\Sigma(2,3)}_{\textbf{Self-energy}}G_1(3,1')$$

Self-energy

$$\int d3\Sigma(2,3)G_1(3,1') = -i\int d3v(2,3)G_2(23,1'3^+)$$

Dynamical equation for G_1

$$G_1(1,1') = G_0(1,1') - i\int d2d3G_0(1,2)v(2,3)G_2(23;1'3^+)$$

Dyson equation

$$G_1(1,1') = G_0(1,1') + \int d2d3G_0(1,2)\ \underbrace{\Sigma(2,3)}_{\textbf{Self-energy}}\ G_1(3,1')$$

Self-energy

$$\int d1'd3\Sigma(2,3)G_1(3,1')G_1^{-1}(1',4) = -i\int d1'd3v(2,3)G_2(23,1'3^+)G_1^{-1}(1',4)$$

Dynamical equation for G_1

$$G_1(1,1') = G_0(1,1') - i\int d2d3G_0(1,2)v(2,3)G_2(23;1'3^+)$$

Dyson equation

$$G_1(1,1') = G_0(1,1') + \int d2d3G_0(1,2)\underbrace{\Sigma(2,3)}_{\textbf{Self-energy}}G_1(3,1')$$

Self-energy

$$\int d1'd3\Sigma(2,3)\overbrace{G_1(3,1')G_1^{-1}(1',4)}^{\delta(3,4)} = -i\int d1'd3v(2,3)G_2(23,1'3^+)G_1^{-1}(1',4)$$

Dynamical equation for G_1

$$G_1(1,1') = G_0(1,1') - i\int d2d3G_0(1,2)v(2,3)G_2(23;1'3^+)$$

Dyson equation

$$G_1(1,1') = G_0(1,1') + \int d2d3G_0(1,2)\underbrace{\Sigma(2,3)}_{\textbf{Self-energy}}G_1(3,1')$$

Self-energy

$$\Sigma(2,3) = -i\int d4d5v(2,4)G_2(24,54^+)G_1^{-1}(5,3)$$

Self-energy

$$\Sigma(2,3) = -i \int d4d5v(2,4)G_2(24,54^+)G_1^{-1}(5,3)$$

- Self-energy is exactly determined starting from a two-body interaction.
- G_2 is connected to G_1 and G_3 and so on...

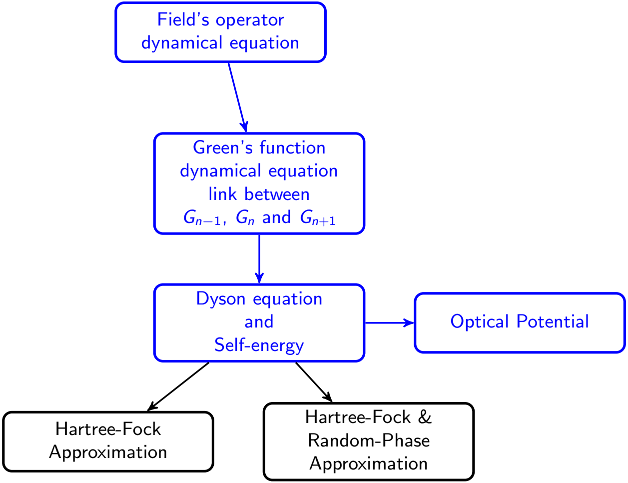
Field's operator
dynamical equation
Green's function
dynamical equation
link between
G_{n-1}, G_n and G_{n+1}
Dyson equation
and
Self-energy
Optical Potential
Hartree-Fock
Approximation
Hartree-Fock &
Random-Phase
Approximation

Dyson equation

$$G_1(1,1') = G_0(1,1') - \int d2d3\, G_0(1,2)\Sigma(2,3)G_1(3,1')$$

Dyson equation

$$G_1(1,1') = G_0(1,1') - \int d2d3 G_0(1,2)\Sigma(2,3)G_1(3,1')$$

$$\left(\frac{\partial}{\partial t} + \frac{1}{2m}\Delta\right) \mapsto \text{Dyson equation}$$

$$\left(\frac{\partial}{\partial t} + \frac{1}{2m}\Delta\right) G_1(x,x') = \delta(x,x') - \int dx''\Sigma(x,x'')G_1(x'',x')$$

Dyson equation

$$G_1(1,1') = G_0(1,1') - \int d2d3G_0(1,2)\Sigma(2,3)G_1(3,1')$$

$$\left(\frac{\partial}{\partial t} + \frac{1}{2m}\Delta\right) \mapsto \text{Dyson equation}$$

$$\left(\frac{\partial}{\partial t} + \frac{1}{2m}\Delta\right) G_1(x,x') = \delta(x,x') - \int dx''\Sigma(x,x'')G_1(x'',x')$$

$$\text{FT}\left[\left(\frac{\partial}{\partial t} + \frac{1}{2m}\Delta\right) \mapsto \text{Dyson equation}\right]$$

$$\left(\varepsilon - \frac{p^2}{2m}\right) G_1(\mathbf{r},\mathbf{r'};\varepsilon) = \delta(\mathbf{r},\mathbf{r'}) - \int d\mathbf{r''}\Sigma(\mathbf{r},\mathbf{r''};\varepsilon)G_1(\mathbf{r''},\mathbf{r'};\varepsilon)$$

$$\mathrm{FT}\left[\left(\frac{\partial}{\partial t}+\frac{1}{2m}\Delta\right)\mapsto \text{Dyson equation}\right]$$

$$\left(\varepsilon-\frac{p^2}{2m}\right)G_1(\mathbf{r},\mathbf{r'};\varepsilon)=\delta(\mathbf{r},\mathbf{r'})-\int d\mathbf{r''}\Sigma(\mathbf{r},\mathbf{r''};\varepsilon)G_1(\mathbf{r''},\mathbf{r'};\varepsilon)$$

One-body Green's function

$$G_1(x,x')=-i\langle 0|\mathcal{T}(\psi(x)\psi^\dagger(x'))|0\rangle$$

Field's operators

$$\psi^\dagger(x) = \sum_\lambda \phi^*_\lambda(\mathbf{r})a^\dagger_\lambda(t)$$
$$\psi(x) = \sum_\lambda \phi_\lambda(\mathbf{r})a_\lambda(t)$$

$$\mathrm{FT}\left[\left(\frac{\partial}{\partial t}+\frac{1}{2m}\Delta\right)\mapsto \text{Dyson equation}\right]$$

$$\left(\varepsilon-\frac{p^2}{2m}\right)G_1(\mathbf{r},\mathbf{r}';\varepsilon)=\delta(\mathbf{r},\mathbf{r}')-\int d\mathbf{r}''\Sigma(\mathbf{r},\mathbf{r}'';\varepsilon)G_1(\mathbf{r}'',\mathbf{r}';\varepsilon)$$

One-body Green's function

$$G_1(x,x')=\sum_{\lambda\lambda'}\phi_\lambda(\mathbf{r})\phi^*_{\lambda'}(\mathbf{r}')G_{\lambda\lambda'}(t-t')$$

Field's operators

$$\begin{aligned}\psi^\dagger(x) &= \sum_\lambda \phi^*_\lambda(\mathbf{r})a^\dagger_\lambda(t)\\ \psi(x) &= \sum_\lambda \phi_\lambda(\mathbf{r})a_\lambda(t)\end{aligned}$$

$$\mathrm{FT}\left[\left(\frac{\partial}{\partial t}+\frac{1}{2m}\Delta\right)\mapsto \text{Dyson equation}\right]$$

$$\left(\varepsilon-\frac{p^2}{2m}\right)G_1(\mathbf{r},\mathbf{r'};\varepsilon)=\delta(\mathbf{r},\mathbf{r'})-\int d\mathbf{r''}\Sigma(\mathbf{r},\mathbf{r''};\varepsilon)G_1(\mathbf{r''},\mathbf{r'};\varepsilon)$$

$\mathrm{FT}(G_1)$

$$G_1(\mathbf{r},\mathbf{r'};\varepsilon)=\sum_{\lambda\lambda'}\phi_\lambda(\mathbf{r})\phi^*_{\lambda'}(\mathbf{r'})G_{\lambda\lambda'}(\varepsilon)$$

Field's operators

$$\begin{aligned}\psi^\dagger(x) &= \sum_\lambda \phi^*_\lambda(\mathbf{r})a^\dagger_\lambda(t)\\ \psi(x) &= \sum_\lambda \phi_\lambda(\mathbf{r})a_\lambda(t)\end{aligned}$$

$$\mathrm{FT}\left[\left(\frac{\partial}{\partial t}+\frac{1}{2m}\Delta\right)\mapsto \text{Dyson equation}\right]$$

$$\left(\varepsilon-\frac{p^2}{2m}\right)\sum_{\lambda\lambda'}\phi_\lambda(\mathbf{r})\phi^*_{\lambda'}(\mathbf{r'})G_{\lambda\lambda'}(\varepsilon)=\delta(\mathbf{r},\mathbf{r'})$$

$$-\int d\mathbf{r''}\Sigma(\mathbf{r},\mathbf{r''};\varepsilon)\sum_{\lambda\lambda'}\phi_\lambda(\mathbf{r})\phi^*_{\lambda'}(\mathbf{r'})G_{\lambda\lambda'}(\varepsilon)$$

$\mathrm{FT}(G_1)$

$$G_1(\mathbf{r},\mathbf{r'};\varepsilon)=\sum_{\lambda\lambda'}\phi_\lambda(\mathbf{r})\phi^*_{\lambda'}(\mathbf{r'})G_{\lambda\lambda'}(\varepsilon)$$

Field's operators

$$\begin{aligned}\psi^\dagger(x) &= \sum_\lambda \phi^*_\lambda(\mathbf{r})a^\dagger_\lambda(t)\\ \psi(x) &= \sum_\lambda \phi_\lambda(\mathbf{r})a_\lambda(t)\end{aligned}$$

$$\mathrm{FT}\left[\left(\frac{\partial}{\partial t}+\frac{1}{2m}\Delta\right)\mapsto \text{Dyson equation}\right]$$

$$\left(\varepsilon-\frac{p^2}{2m}\right)\sum_{\lambda\lambda'}\phi_\lambda(\mathbf{r})\phi^*_{\lambda'}(\mathbf{r'})G_{\lambda\lambda'}(\varepsilon)=\delta(\mathbf{r},\mathbf{r'}) - \int d\mathbf{r''}\,\Sigma(\mathbf{r},\mathbf{r''};\varepsilon)\sum_{\lambda\lambda'}\phi_\lambda(\mathbf{r})\phi^*_{\lambda'}(\mathbf{r'})G_{\lambda\lambda'}(\varepsilon)$$

$$\int d\mathbf{r}d\mathbf{r'}\phi^*_{\lambda_3}(\mathbf{r})\phi_{\lambda_4}(\mathbf{r'})\mathrm{FT}\left[\left(\frac{\partial}{\partial t}+\frac{1}{2m}\Delta\right)\mapsto \text{Dyson equation}\right]$$

$$\sum_{\lambda_1}\left\{\varepsilon\delta_{\lambda_1\lambda_3}-\int d\mathbf{r}\phi^*_{\lambda_3}(\mathbf{r})\frac{p^2}{2m}\phi_{\lambda_1}(\mathbf{r}) + \int d\mathbf{r}\phi^*_{\lambda_3}(\mathbf{r})\int d\mathbf{r''}\,\Sigma(\mathbf{r},\mathbf{r''};\varepsilon)\phi_{\lambda_1}(\mathbf{r''})\right\}G_{\lambda_1\lambda_4}(\varepsilon)=\delta_{\lambda_3\lambda_4}$$

$$\int d\mathbf{r}d\mathbf{r'}\phi^*_{\lambda_3}(\mathbf{r})\phi_{\lambda_4}(\mathbf{r'})\mathrm{FT}\left[\left(\frac{\partial}{\partial t}+\frac{1}{2m}\Delta\right)\mapsto \text{Dyson equation}\right]$$

$$\sum_{\lambda_1}\left\{\varepsilon\delta_{\lambda_1\lambda_3}-\int d\mathbf{r}\phi^*_{\lambda_3}(\mathbf{r})\frac{p^2}{2m}\phi_{\lambda_1}(\mathbf{r})\right.$$
$$\left.+\int d\mathbf{r}\phi^*_{\lambda_3}(\mathbf{r})\int d\mathbf{r''}\Sigma(\mathbf{r},\mathbf{r''};\varepsilon)\phi_{\lambda_1}(\mathbf{r''})\right\}G_{\lambda_1\lambda_4}(\varepsilon)=\delta_{\lambda_3\lambda_4}$$

Let's consider a set of wave functions ϕ_λ that diagonalizes it

$$[\varepsilon-E_\lambda(\varepsilon)]\,G_{\lambda\lambda'}(\varepsilon)=\delta_{\lambda\lambda'}$$

hence

$$\langle\lambda_3|\frac{p^2}{2m}+\int d\mathbf{r''}\Sigma(\mathbf{r},\mathbf{r''};\varepsilon)|\lambda_1\rangle=E_{\lambda_1}(\varepsilon)\delta_{\lambda_3\lambda_1}$$

The set of wave functions ϕ_λ obeys

$$\frac{p^2}{2m}\phi_\lambda(\mathbf{r})+\int d\mathbf{r''}\Sigma(\mathbf{r},\mathbf{r''};\varepsilon)\phi_\lambda(\mathbf{r''})=E_\lambda(\varepsilon)\phi_\lambda(\mathbf{r})$$

Schrödinger equation

$$\frac{p^2}{2m}\phi_\lambda(\mathbf{r},\varepsilon) + \int d\mathbf{r'}\Sigma(\mathbf{r},\mathbf{r'};\varepsilon)\phi_\lambda(\mathbf{r'},\varepsilon) = E(\varepsilon)\phi_\lambda(\mathbf{r},\varepsilon)$$

Schrödinger equation

$$\frac{p^2}{2m}\phi_\lambda(\mathbf{r},\varepsilon) + \int d\mathbf{r'}\Sigma(\mathbf{r},\mathbf{r'};\varepsilon)\phi_\lambda(\mathbf{r'},\varepsilon) = E(\varepsilon)\phi_\lambda(\mathbf{r},\varepsilon)$$

$\rightarrow$ **ϕ's are the wave functions of a particle experiencing a potential Σ which is nonlocal and energy dependent**

Schrödinger equation

$$\frac{p^2}{2m}\phi_\lambda(\mathbf{r},\varepsilon) + \int d\mathbf{r'}\Sigma(\mathbf{r},\mathbf{r'};\varepsilon)\phi_\lambda(\mathbf{r'},\varepsilon) = E(\varepsilon)\phi_\lambda(\mathbf{r},\varepsilon)$$

→ **ϕ's are the wave functions of a particle experiencing a potential Σ which is nonlocal and energy dependent**

→ **Optical potential is connected to the Fourier transform of Self-energy itself connected to the two-body interaction.**

Schrödinger equation

$$\frac{p^2}{2m}\phi_\lambda(\mathbf{r},\varepsilon)+\int d\mathbf{r'}\Sigma(\mathbf{r},\mathbf{r'};\varepsilon)\phi_\lambda(\mathbf{r'},\varepsilon)=E(\varepsilon)\phi_\lambda(\mathbf{r},\varepsilon)$$

→ **ϕ's are the wave functions of a particle experiencing a potential Σ which is nonlocal and energy dependent**

→ **Optical potential is connected to the Fourier transform of Self-energy itself connected to the two-body interaction.**

→ **At that level of the calculation there is no average on the energy**

→ **The calculation is formaly complete: direct, preequilibrium, CN ...**

Road map

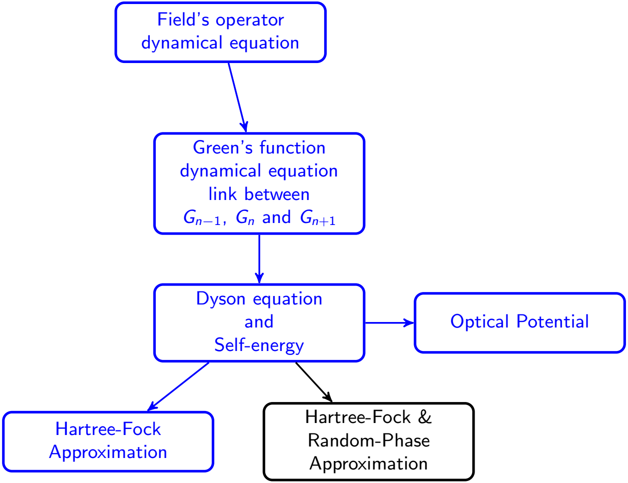
Field's operator dynamical equation
Green's function dynamical equation link between G_{n-1}, G_n and G_{n+1}
Dyson equation and Self-energy
Optical Potential
Hartree-Fock Approximation
Hartree-Fock & Random-Phase Approximation

Dynamical equation for G_1

$$G_1(1,1') = G_0(1,1') - i\int d2d3 G_0(1,2)v(2,3)G_2(23,1'3^+)$$

Hartree-Fock approximation

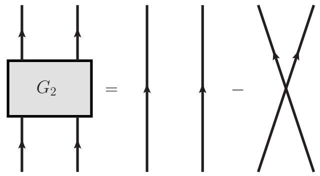

1. Two-body correlations are neglected
2. G_2 becomes an antisymmetrized product of G_1's

Dynamical equation for G_1 within HF approximation

$$G_1^{HF}(1,1') \;=\; G_0(1,1') - i\int d2d3 G_0(1,2)v(2,3)\left(G_1^{HF}(2,1')G_1^{HF}(3,3^+) - G_1^{HF}(2,3^+)G_1^{HF}(3,1')\right)$$

Dynamical equation for G_1 within HF approximation

$$G_1^{HF}(1,1') = G_0(1,1') - i\int d2d3\,G_0(1,2)v(2,3)\left(G_1^{HF}(2,1')G_1^{HF}(3,3^+) - G_1^{HF}(2,3^+)G_1^{HF}(3,1')\right)$$

Hartree-Fock Diagrammatic

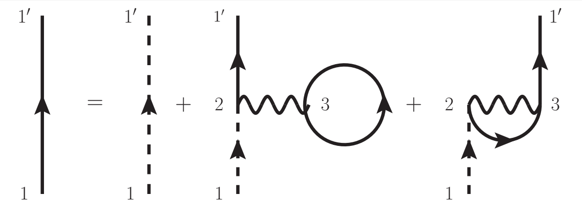

Infinite sum of *'bubbles'* and *'oysters'*

Exact Self-energy

$$\Sigma(2,3) = -i \int d4d5 v(2,4) G_2(24, 54^+) G_1^{-1}(5,3)$$

Self-energy at the HF approximation

$$\Sigma^{HF}(2,3) = -i \int d4d5 v(2,4) \left(G_1(2,5) G_1(4,4^+) - G_1(2,4^+) G_1(4,5) \right) G_1^{-1}(5,3)$$

Exact Self-energy

$$\Sigma(2,3) = -i \int d4d5 v(2,4) G_2(24, 54^+) G_1^{-1}(5,3)$$

Self-energy at the HF approximation

$$\Sigma^{HF}(2,3) = -i \int d4d5 v(2,4) \left(G_1(2,5) G_1(4,4^+) - G_1(2,4^+) G_1(4,5) \right) G_1^{-1}(5,3)$$

Exact Self-energy

$$\Sigma(2,3) = -i \int d4d5 v(2,4) G_2(24, 54^+) G_1^{-1}(5,3)$$

Self-energy at the HF approximation

$$\Sigma^{HF}(2,3) = -i \int d4 v(2,4) \left(\delta(2,3) G_1(4,4^+) - G_1(2,4^+) \delta(4,3) \right)$$

Exact Self-energy

$$\Sigma(2,3) = -i \int d4d5 v(2,4) G_2(24, 54^+) G_1^{-1}(5,3)$$

Self-energy at the HF approximation

$$\Sigma^{HF}(2,3) = -i \int d4 v(2,4)\delta(2,3) G_1(4,4^+) + i\ v(2,3) G_1(2,3)$$

Exact Self-energy

$$\Sigma(2,3) = -i \int d4d5v(2,4)G_2(24,54^+)G_1^{-1}(5,3)$$

Self-energy at the HF approximation

$$\Sigma^{HF}(2,3) = -i \int d4v(2,4)\delta(2,3)G_1(4,4^+) + i\ v(2,3)G_1(2,3)$$

Schrödinger equation

$$\frac{p^2}{2m}\phi_\lambda(\mathbf{r},\varepsilon) + \int d\mathbf{r'}\ \underbrace{\Sigma^{HF}(\mathbf{r},\mathbf{r'};\varepsilon)}_{\textbf{FT of Self-energy}}\ \phi_\lambda(\mathbf{r'},\varepsilon) = E(\varepsilon)\phi_\lambda(\mathbf{r},\varepsilon)$$

Self-energy at the HF approximation

$$\Sigma^{HF}(2,3) = -i \int d4 v(2,4)\delta(2,3)G_1(4,4^+) + i\ v(2,3)G_1(2,3)$$

One-body Green's function

$$G_1(x,x') = \sum_{\lambda\lambda'} \phi_\lambda(\mathbf{r})\phi^*_{\lambda'}(\mathbf{r'})G_{\lambda\lambda'}(t-t')$$

Occupation numbers

$$G_{\lambda\lambda}(t-t'=+0) = -i(1-m_\lambda)$$
$$G_{\lambda\lambda}(t-t'=-0) = i\ m_\lambda$$
$$m_\lambda = \langle\psi_0|a^\dagger_\lambda a_\lambda|\psi_0\rangle$$

Fourier transform of Σ^{HF} with $v(x,x') = v(\mathbf{r}-\mathbf{r'})\delta(t-t')$

$$\begin{aligned}
\Sigma^{HF}(\mathbf{r},\mathbf{r''};\varepsilon) &= \delta(\mathbf{r},\mathbf{r''})\int d\mathbf{r'} v(\mathbf{r},\mathbf{r'})\sum_\lambda m_\lambda \phi^*_\lambda(\mathbf{r'})\phi_\lambda(\mathbf{r'}) \\
&- v(\mathbf{r},\mathbf{r''})\sum_\lambda m_\lambda \phi^*_\lambda(\mathbf{r})\phi_\lambda(\mathbf{r''}) \\
&= \delta(\mathbf{r},\mathbf{r''})\int d\mathbf{r'} v(\mathbf{r},\mathbf{r'})\rho(\mathbf{r'}) - v(\mathbf{r},\mathbf{r''})\rho(\mathbf{r},\mathbf{r''})
\end{aligned}$$

Schrödinger equation

$$\frac{p^2}{2m}\phi_\lambda(\mathbf{r},\varepsilon) + \int d\mathbf{r'}\, V^{HF}(\mathbf{r},\mathbf{r'};\varepsilon)\phi_\lambda(\mathbf{r'},\varepsilon) = E(\varepsilon)\phi_\lambda(\mathbf{r},\varepsilon)$$

HF potential

$$V^{HF}(\mathbf{r},\mathbf{r''};\varepsilon) = \delta(\mathbf{r},\mathbf{r''})\int d\mathbf{r'}\, v(\mathbf{r},\mathbf{r'})\rho(\mathbf{r'}) - v(\mathbf{r},\mathbf{r''})\rho(\mathbf{r},\mathbf{r''})$$

$$\begin{tikzcd} \rho \arrow[rr, bend left, "\text{NN interaction}"] & & V^{HF}(\rho) \arrow[ll, bend left, "\text{Schrödinger equation}"] \end{tikzcd}$$

Schrödinger equation

$$\frac{p^2}{2m}\phi_\lambda(\mathbf{r},\varepsilon) + \int d\mathbf{r}' V^{HF}(\mathbf{r},\mathbf{r}';\varepsilon)\phi_\lambda(\mathbf{r}',\varepsilon) = E(\varepsilon)\phi_\lambda(\mathbf{r},\varepsilon)$$

HF potential

$$V^{HF}(\mathbf{r},\mathbf{r}'';\varepsilon) = \delta(\mathbf{r},\mathbf{r}'')\int d\mathbf{r}' v(\mathbf{r},\mathbf{r}')\rho(\mathbf{r}') - v(\mathbf{r},\mathbf{r}'')\rho(\mathbf{r},\mathbf{r}'')$$

$$\begin{tikzcd}
\rho \arrow[r, bend left, "\text{NN interaction}"] & V^{HF}(\rho) \arrow[l, bend left, "\text{Schrödinger equation}"]
\end{tikzcd}$$

If the 2-body interaction is finite range, the HF potential is nonlocal

HF potential shape

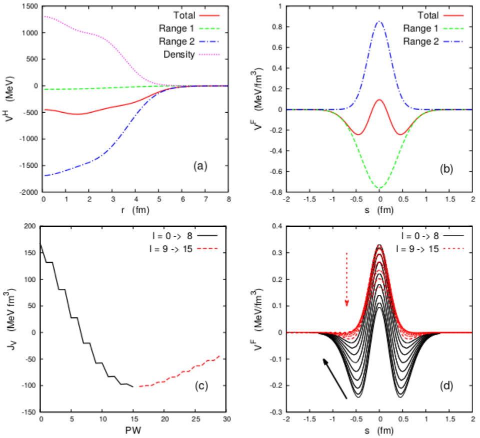

Fig. 15. Contributions for n + ^{40}Ca to: (a) to the Hartree local potential (V^H): Total (solid line), first range of D1S (dashed line), second range of D1S (dash-dotted line) and density term (dotted line). (b) First partial wave of the nonlocal Fock term at $r = r' = 4.3$ fm: Total (solid line), first range of D1S (dashed line) and second range of D1S (dash-dotted line). (c) Volume integral of the Fock potential as a function of partial wave: Negative slope (solid line), positive slope (dashed line). (d) Same as

Scattering off a mean-field potential

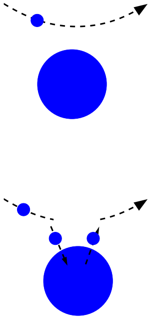

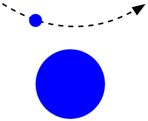

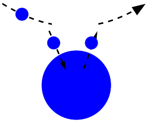

Numerical resolution of the scattering equation with V_{HF}

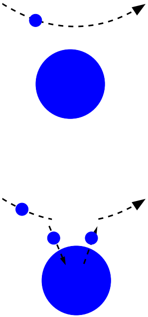

Numerical resolution of the scattering equation with V_{HF}

$\rightarrow$ **Matching**

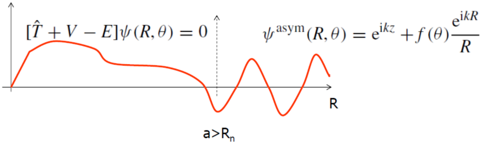

R_n : some large R where $V(R) \approx 0$ (potential dependent)

Scattering off a mean-field potential

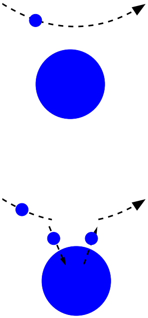

Numerical resolution of the scattering equation with V_{HF}

$\rightarrow$ Matching

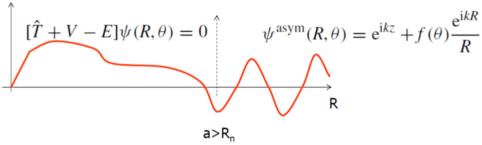

R_n : some large R where $V(R) \approx 0$ (potential dependent)

$\rightarrow$ Phaseshift δ_{lj}

HF phaseshift n/p+^{40}Ca

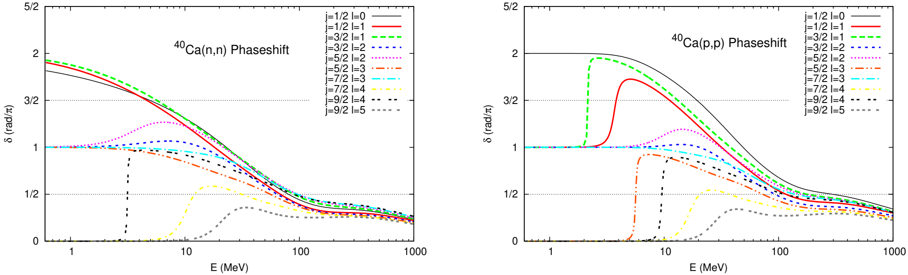

- Single particle resonances when $\delta = n\pi/2$ (n impair).
- Levinson theorem and total cross section

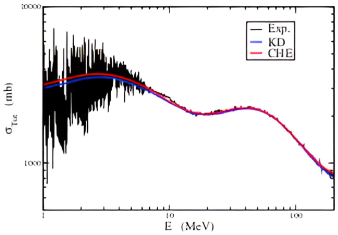

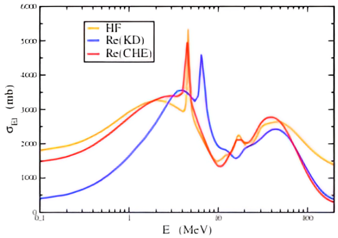

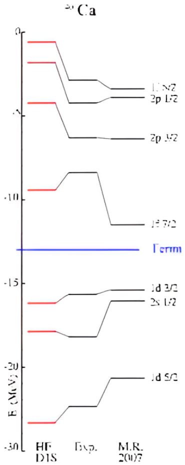

- V^{HF} gives the main contribution to the real part of the potential

(B. Morillon and P. Romain, Phys. Rev. C 70, 014601 (2004).) → dispersive potential

(A. J. Koning and J. P. Delaroche, Nuclear Physics A 713, 231 (2003).)

HF differential cross section

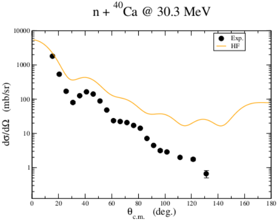

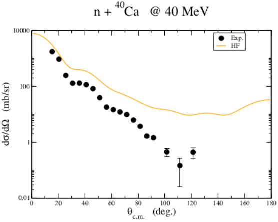

HF differential cross section

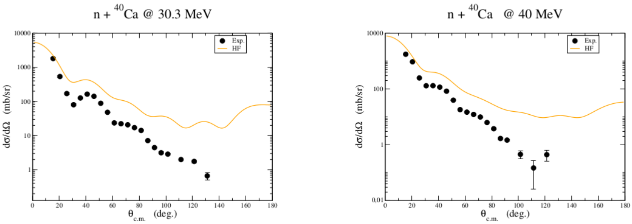

→ Cross section is overpredicted

→ Lack of absorption

→ Need to account for more inelastic processes

Road map

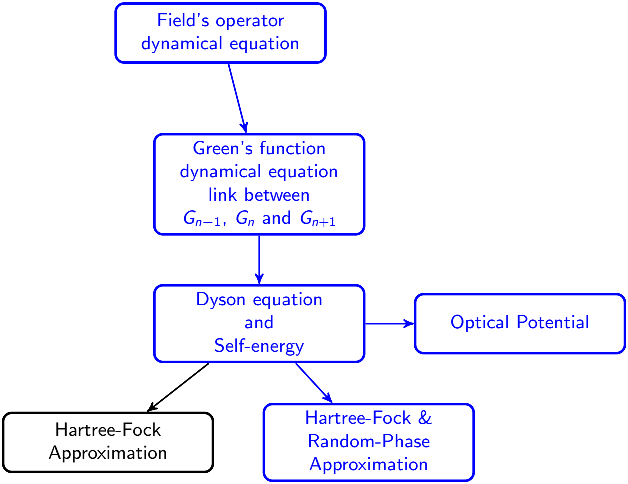

Field's operator dynamical equation
Green's function dynamical equation link between G_{n-1}, G_n and G_{n+1}
Dyson equation and Self-energy
Optical Potential
Hartree-Fock Approximation
Hartree-Fock & Random-Phase Approximation

Exact Self-energy

$$\Sigma(2,3) = -i \int d4d5 v(2,4) G_2(24, 54^+) G_1^{-1}(5,3)$$

Exact Self-energy

$$\Sigma(2,3) = -i \int d4d5 v(2,4) G_2(24, 54^+) G_1^{-1}(5,3)$$

Let's go directly to the result...

Self-energy at the HF+RPA approximation

$$
\begin{aligned}
\Sigma_1(1,1') &= \Sigma_{HF}(1,1') + \Sigma_{pp}(1,1') + \Sigma_{ph}(1,1') - 2\Sigma^{(2)}(1,1') \\
\Sigma_{HF}(1,1') &= iv(1,1')G_1^{HF}(1,1') - i\delta(1,1')\int d2v(1,2)G_1^{HF}(2;2^+) \\
\Sigma_{pp}(1,1') &= \int d3d4v(1,3)G_1^{HF}(4,3)G_2(13;1'4)v(4,1') \\
\Sigma_{ph}(1,1') &= -\int d3d4v(1,3)\left[G_1^{HF}(1,1')G_2(34;3^+4^+)\right. \\
&\quad -G_1^{HF}(1,4)G_2(43;1'3^+) - G_1^{HF}(3,1')G_2(41;4^+3) \\
&\quad \left. -\; G_1^{HF}(3,4)G_2(14;1'3)\right] v(4,1')
\end{aligned}
$$

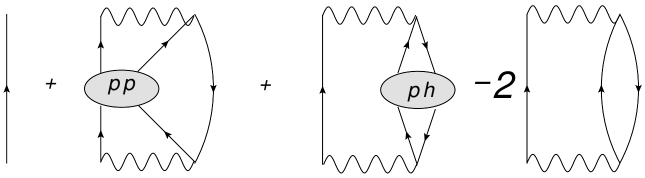

Schrödinger equation

$$\frac{p^2}{2m}\phi_\lambda(\mathbf{r},\varepsilon) + \int d\mathbf{r'}V^{HF}(\mathbf{r},\mathbf{r'};\varepsilon)\phi_\lambda(\mathbf{r'},\varepsilon) = E(\varepsilon)\phi_\lambda(\mathbf{r},\varepsilon)$$

HF potential

$$V^{HF}(\mathbf{r},\mathbf{r''};\varepsilon) = \delta(\mathbf{r},\mathbf{r''})\int d\mathbf{r'}v(\mathbf{r},\mathbf{r'})\rho(\mathbf{r'}) - v(\mathbf{r},\mathbf{r''})\rho(\mathbf{r},\mathbf{r''})$$

RPA potential

$$\begin{aligned} V^{RPA}(\mathbf{r},\mathbf{r}',E) &= \lim_{\eta\to 0^+}\sum_{N\neq 0}\sum_{ijk\lambda}\!\!\!\!\!\!\!\int \chi_{ij}^{(N)}\chi_{kl}^{(N)} \\ &\times \left(\frac{n_\lambda}{E-\epsilon_\lambda+E_N-i\eta} + \frac{1-n_\lambda}{E-\epsilon_\lambda-E_N+i\eta}\right) \\ &\times F_{ij\lambda}(\mathbf{r})F^*_{kl\lambda}(\mathbf{r}') \end{aligned}$$

with

$$F_{ij\lambda}(\mathbf{r}) = \int d^3\mathbf{r}_1\phi_i^*(\mathbf{r}_1)v(\mathbf{r},\mathbf{r}_1)[1-P]\phi_\lambda(\mathbf{r})\phi_j(\mathbf{r}_1)$$

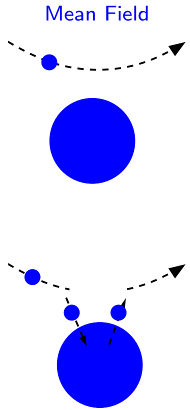
Mean Field

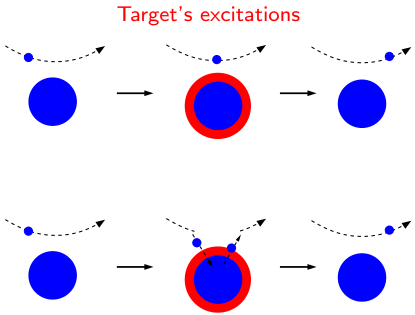
Target's excitations

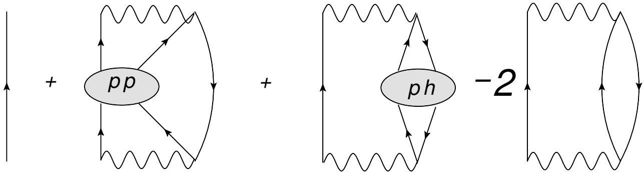
+
pp
+
ph
−2

Complex RPA potential

$$
\begin{aligned}
V_{RPA}(\mathbf{r},\mathbf{r}',E) &= \lim_{\eta\to 0^+} \sum_{N\neq 0,\, ijkl} \sum_{\lambda} \int \chi_{ij}^{(N)} \chi_{kl}^{(N)} \\
&\times \left(\frac{n_\lambda}{E-\epsilon_\lambda+E_N-i\eta} + \frac{1-n_\lambda}{E-\epsilon_\lambda-E_N+i\eta} \right) F_{ij\lambda}(\mathbf{r}) F_{kl\lambda}^{*}(\mathbf{r}')
\end{aligned}
$$

Plemelj formula $\lim_{\eta\to 0^+} \int_a^b \frac{f(x)}{x-x_0\mp i\eta}dx = \mathscr{P}\int_a^b \frac{f(x)}{x-x_0}dx \pm i\pi f(x_0)$

$$
\begin{aligned}
\lim_{\eta\to 0^+} \int \frac{-(1-n_\lambda) f^{(ijkl,N)}(\epsilon_\lambda)}{\epsilon_\lambda-(E-E_N)-i\eta} d\epsilon_\lambda &= \mathscr{P}\int \frac{-(1-n_\lambda) f^{(ijkl,N)}(\epsilon_\lambda)}{\epsilon_\lambda-(E-E_n)} d\epsilon_\lambda \\
&- (1-n_\lambda) i\pi \int f^{(ijkl,N)}(\epsilon_\lambda)\delta(\epsilon_\lambda-(E-E_N)) d\epsilon_\lambda
\end{aligned}
$$

- When $\eta \to 0$, only $E_N < E$ excitations contribute to the imaginary part of the RPA potential.
- When $\eta \to 0$, no contribution from the *compound nucleus* terms to the absorption ($\sum_\lambda$).
- The determination of the real part requires all the excitations.

Effect of HF intermediate propagator

- $p+^{40}Ca$
- $V_{HF} + \mathrm{Im}(V_{RPA})$
- Coupling to the first 1^- $E_{1-} = 9.7 MeV$

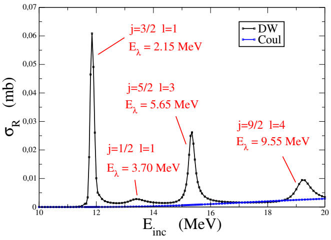

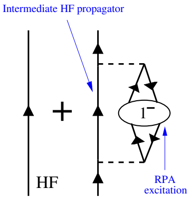

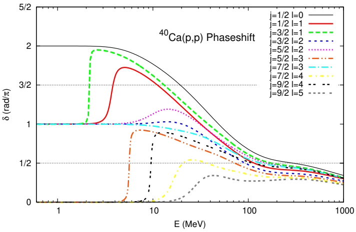

- Effect of resonances of the intermediate HF propagator.
- Enhancement of σ_R compared as with a Coulomb wave.

$$\lim_{\eta\to 0^+} \int Im\left(\frac{-(1-n_\lambda) f^{(ijkl,N)}(\epsilon_\lambda)}{\epsilon_\lambda - (E-E_n) - i\eta}\right) d\epsilon_\lambda = -(1-n_\lambda)\pi \int f^{(ijkl,N)}(\epsilon_\lambda)\delta(\epsilon_\lambda - (E-E_n)) d\epsilon_\lambda$$

Effect of HF intermediate propagator

- σ_R from $V_{HF} + \mathrm{Im}(V_{RPA})$
- σ_R from $V_{HF} + \mathrm{Im}(V_{PH})$

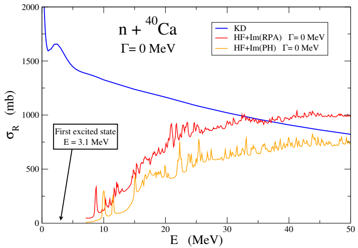

$\rightarrow$ Effect of the HF resonances on $\mathrm{Im}(V_{RPA})$

- Zero width calculation:
  - $\sigma_R = 0$ for incident energies below the energy of the first excited state of the target nucleus
- ^{40}Ca RPA states $J = 0 \rightarrow 8$

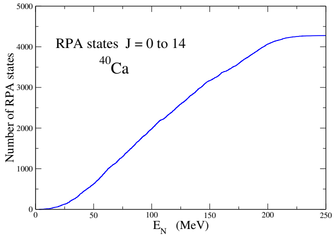

$$\lim_{\eta \to 0^+} \int \frac{-(1-n_\lambda) f^{(ijkl,N)}(\epsilon_\lambda)}{\epsilon_\lambda - (E - E_n) - i\eta} d\epsilon_\lambda = \mathscr{P} \int \frac{-(1-n_\lambda) f^{(ijkl,N)}(\epsilon_\lambda)}{\epsilon_\lambda - (E - E_n)} d\epsilon_\lambda - (1-n_\lambda) i\pi \int f^{(ijkl,N)}(\epsilon_\lambda)\delta(\epsilon_\lambda - (E - E_n)) d\epsilon_\lambda$$

Effect of HF intermediate propagator

- σ_R from $V_{HF} + \mathrm{Im}(\Delta V_{RPA})$

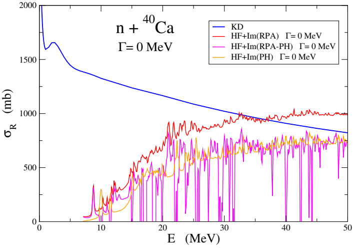

- In this work
  - Consistent scheme (Gogny interaction only)
  - Use of a phenomenological width (Harakeh and van der Woude)

- Physical origin of width
  - Self-consistent scheme
  - $\eta \neq 0$ when HF propagator gets dressed by RPA
  - $E_N \rightarrow E_N + i\Gamma_N(E_N)$

    Damping (doorway state) & continuum

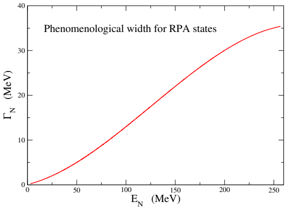

Dispersion relation

Causality $\rightarrow$ relation between real and imaginary parts

$$\begin{aligned} V(E) &= V_R(E) + iV_I(E); \\ V_R(E) &= V_{HF} + \Delta V_R(E), \\ \Delta V_R(E) &= \frac{\mathcal{P}}{\pi} \int_{-\infty}^{+\infty} \frac{V_I(E')}{E' - E} dE'. \end{aligned}$$

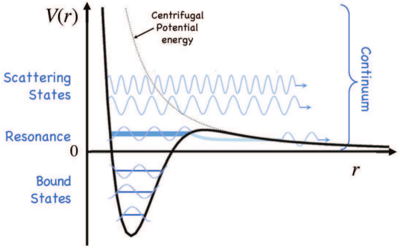

Bound states are taken into account in the determination of the potential

Outline

Phenomenological optical potentials

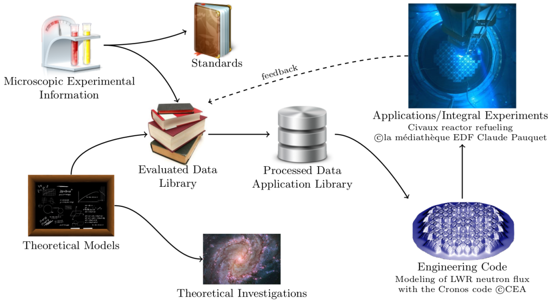

Figure 1.1 – Schematic of the nuclear data path from experimental and/or theoretical sources to industrial applications.

Picture from Tamagno

- Precision required for the evaluations
- Constrained by numerous calculations using reaction codes: TALYS, EMPIRE
- Predictivity outside the range parametrization?
- Parametrization of non local dispersive potentials
- Issues induced by localisation procedures : effet Perey, dépendance spurieuse en énergie

Things we learn from microscopy

We have shown that optical potential is

- Nonlocal $V(\mathbf{r}, \mathbf{r}')$
- Complex $V = U + iW$
- Absorptif $W < 0$
- Energy-dependent $V(\mathbf{r}, \mathbf{r}', E)$
- Dispersive

$$V(E) = V_{HF} + \Delta\, V(E),$$

$$\Delta\, V(E) = \frac{P}{\pi} \int_{-\infty}^{+\infty} \frac{W(E')}{E' - E} dE',$$

where P denotes the principal value of the integral.

Outline

Origin of nonlocality

- **Antisymmetrization**

$$V_{HF}(\mathbf{r},\mathbf{r'}) = \int d\mathbf{r}_1 \rho(\mathbf{r}_1) v(\mathbf{r},\mathbf{r}_1) - \rho(\mathbf{r},\mathbf{r'}) v(\mathbf{r},\mathbf{r'})$$

Origin of nonlocality

- **Antisymmetrization**

$$V_{HF}(\mathbf{r},\mathbf{r'}) = \int d\mathbf{r}_1 \rho(\mathbf{r}_1) v(\mathbf{r},\mathbf{r}_1) - \rho(\mathbf{r},\mathbf{r'}) v(\mathbf{r},\mathbf{r'})$$

- **Polarization (Second order diagrams)**
  Surface term...

$$\Delta U(\mathbf{r},\mathbf{r}';E) = \sum_i V_{0i}(\mathbf{r}) G_{ii}(\mathbf{r},\mathbf{r'};E) V_{i0}(\mathbf{r'}),$$

where G_{ii} is a propagator

$$V_{i0}(\mathbf{r}) = \beta_i r \frac{dU(r)}{dr} Y_\lambda^\mu(\widehat{\mathbf{r}}),$$

transition potential in the Bohr collective model.

A. Lev, W. P. Beres, and M. Divadeenam. PRC 9 :2416–2434, Jun 1974.

$$V(r) = -[V_0 + iW_I] f_{vol}(r) - iW_D f_{surf}(r) - (U_{so} + iW_{so}) f_{surf}(r)\, \ell \cdot \boldsymbol{\sigma}$$

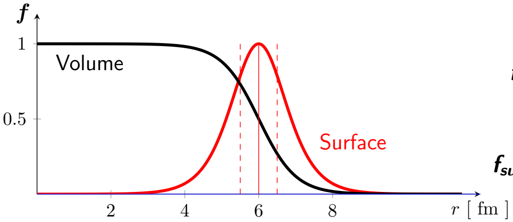

$$f_{vol}(r) \sim \frac{1}{1 + e^{(r - R_0)/a}}$$

$$f_{surf}(r) \sim \frac{4\, e^{(r - R_0)/a}}{[1 + e^{(r - R_0)/a}]^2}$$

Integro-differential equation,

$$-\frac{\hbar^2}{2\mu}\Delta\psi(\mathbf{r}) + \int V_{NL}(\mathbf{r},\mathbf{r'})\psi(\mathbf{r'})\mathrm{d}\mathbf{r'} = E\psi(\mathbf{r}),$$

with μ the reduced mass. A local potential reads,

$$V_{NL}(\mathbf{r},\mathbf{r'}) = V_L(\mathbf{r})\delta(\mathbf{r},\mathbf{r'}).$$

and the equation is **differential**,

$$-\frac{\hbar^2}{2\mu}\Delta\psi(\mathbf{r}) + V_L(\mathbf{r})\psi(\mathbf{r}) = E\psi(\mathbf{r}).$$

$\rightarrow$ **Modernisation of the numerical tools**

ELSEVIER

Available online at www.sciencedirect.com

SCIENCE DIRECT®

Nuclear Physics A 713 (2003) 231–310

NUCLEAR PHYSICS A

www.elsevier.com/locate/npe

Local and global nucleon optical models from 1 keV to 200 MeV

A.J. Koning [a,*], J.P. Delaroche [b]

[a] *Nuclear Research and Consultancy Group NRG, PO Box 25, 1755 ZG Petten, The Netherlands*
[b] *Commissariat à l'Energie Atomique, DAM/DIF/DPTA, Boîte Postale 12, 91680 Bruyères-le-Châtel, France*

Received 7 August 2002; received in revised form 24 September 2002; accepted 2 October 2002

Koning-Delaroche potential

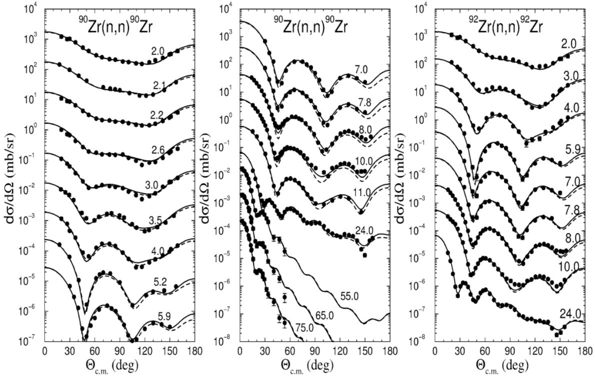

Fig. 17. Comparison of predicted differential cross sections and experimental data, for neutrons scattered from ^{90}Zr and ^{92}Zr. For more details, see Section 4.1.

Local dispersive potential

PHYSICAL REVIEW C **70**, 014601 (2004)

Dispersive and global spherical optical model with a local energy approximation for the scattering of neutrons by nuclei from 1 keV to 200 MeV

B. Morillon and P. Romain
Commissariat à l'Énergie Atomique, DAM/DIF/DPTA/SPN, Boîte Postale 12, 91680 Bruyères-le-Châtel, France
(Received 8 March 2004; published 6 July 2004)

We present a global spherical optical model potential for neutrons with incident energies from 1 keV up to 200 MeV containing dispersive terms and a local energy approximation. A comprehensive database for spherical or quasispherical nuclei covering the mass range $24 \leqslant A \leqslant 209$ is used to automatically search on all parameters. A good representation of the entire data set is obtained when both volume and surface potentials share the same energy-independent geometry.

DOI: 10.1103/PhysRevC.70.014601 PACS number(s): 24.10.Ht

Local dispersive potential

In the dispersion relations treatment [6], the real V and imaginary W volume potentials are connected by a dispersion relation

$$V(E) = V_{\mathrm{HF}}(E) + \Delta V(E),$$

$$\Delta V(E) = \frac{P}{\pi}\int_{-\infty}^{+\infty} \frac{W(E')}{E' - E} dE'. \qquad (2)$$

As usual, P denotes the principal value of the integral and $V_{\mathrm{HF}}(E)$ the Hartree-Fock contribution to the mean field.

B. Real potentials

A realistic parametrization of the Hartree-Fock potential was postulated by Perey and Buck [7]. In their work, the nonlocality of $V_{\mathrm{HF}}(\mathbf{r},\mathbf{r}')$ has a Gaussian form

$$V_{\mathrm{HF}}(\mathbf{r},\mathbf{r}') = V(\mathbf{r})\exp(-|\mathbf{r}-\mathbf{r}'|^2/\beta^2),$$

where β is the nonlocality range. The local energy approximation then yields [7]

$$V_{\mathrm{HF}}(E) = V_{\mathrm{HF}}\exp(-\mu\beta^2[E - V_{\mathrm{HF}}(E)]/2\hbar^2), \qquad (6)$$

Outline

Perey-Buck Nonlocal Potential

2.E

Nuclear Physics **32** (1962) 353—380;

A NON-LOCAL POTENTIAL MODEL FOR THE SCATTERING OF NEUTRONS BY NUCLEI

F. PEREY and B. BUCK

Oak Ridge National Laboratory † *Oak Ridge, Tennessee*

Received 25 September 1961

Abstract: An energy independent non-local optical potential for the elastic scattering of neutrons from nuclei is proposed and the wave-equation solved numerically in its full integro-differential form. The non-local kernel is assumed separable into a potential form factor times a Gaussian non-locality. The potential form factor, of argument $\frac{1}{2}(\mathbf{r}+\mathbf{r}')$, is that of a real Saxon form plus an imaginary term having the shape of the derivative of a Saxon form. A real local spin-orbit potential of the usual Thomas form is included. The parameters of the potential obtained solely from the fitting of the differential cross sections for lead at 7 MeV and 14.5 MeV are used unchanged to calculate the elastic differential cross sections, total and reaction cross sections and polarizations on some elements ranging from Al to Pb at various energies from 0.4 MeV to 24 MeV. The S-wave strength functions and the effective scattering radius R' are also calculated with the same parameters. The parameters in the usual notations are: real potential $V = 71$ MeV, $r = 1.22$ fm, $a = 0.65$ fm; surface imaginary potential $W = 15$ MeV, $a = 0.47$ fm; non-locality $\beta = 0.85$ fm; spin-orbit potential, using the nucleon mass in the Thomas form, $U_{so} = 1300$ MeV. The energy independence of the

Mahzoon Nonlocal Potential

PRL **112,** 162503 (2014) PHYSICAL REVIEW LETTERS week ending 25 APRIL 2014

Forging the Link between Nuclear Reactions and Nuclear Structure

M. H. Mahzoon,[1] R. J. Charity,[2] W. H. Dickhoff,[1] H. Dussan,[1] and S. J. Waldecker[3]
[1]*Department of Physics, Washington University, Saint Louis, Missouri 63130, USA*
[2]*Department of Chemistry, Washington University, Saint Louis, Missouri 63130, USA*
[3]*Department of Physics, University of Tennessee, Chattanooga, Tennessee 37403, USA*
(Received 18 December 2013; published 25 April 2014)

A comprehensive description of all single-particle properties associated with the nucleus ^{40}Ca is generated by employing a nonlocal dispersive optical potential capable of simultaneously reproducing all relevant data above and below the Fermi energy. The introduction of nonlocality in the absorptive potentials yields equivalent elastic differential cross sections as compared to local versions but changes the absorption profile as a function of angular momentum suggesting important consequences for the analysis of nuclear reactions. Below the Fermi energy, nonlocality is essential to allow for an accurate representation of particle number and the nuclear charge density. Spectral properties implied by $(e, e'p)$ and $(p, 2p)$ reactions are correctly incorporated, including the energy distribution of about 10% high-momentum nucleons, as experimentally determined by data from Jefferson Lab. These high-momentum nucleons provide a substantial contribution to the energy of the ground state, indicating a residual attractive contribution from higher-body interactions for ^{40}Ca of about 0.64 MeV/A.

- Cutting edge phenomenological potential: nonlocal, dispersive...
- Both reaction and structure observables accounted for in the calibration

One can get the one-body density matrix

$$n_{lj}(r,r') = \frac{1}{\pi}\int_{-\infty}^{\epsilon_F} dE \; \mathrm{Im} G_{lj}(r,r';E)$$

then charge density reads

$$\rho_p = \frac{e}{4\pi}\sum_{lj}(2j+1)n_{lj}(r,r)$$

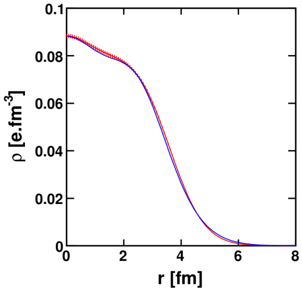

Figure 3.12: Comparison of experimental charge density [28] (thick red hashed line) with the DOM fit (solid blue curve).

Figure from Mahzoon

DOM provides everything constently

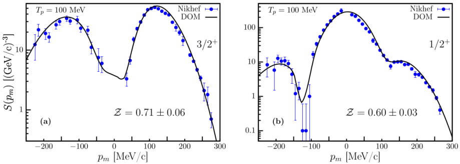

Figure 6. ^{40}Ca$(e, e'p)^{39}$K spectral functions in parallel kinematics, at an outgoing proton kinetic energy of 100 MeV. The solid line is the calculation using the DOM ingredients, while the points are from the experiment detailed in [179]. (a) Distribution for the removal of the $0d\frac{3}{2}$. The curve contains the DWIA for the $3/2^+$ ground state including a spectroscopic factor of 0.71. (b) Distribution for the removal of the $1s\frac{1}{2}$ proton with a spectroscopic factor of 0.60 for the $1/2^+$ excited state at 2.522 MeV. The figure is adapted from figure 5 of [170]. Reprinted with permission from [170], Copyright (2018) by the American Physical Society.

Figure from M.C. Atckinson

- Fit: particle numbers, charge densities, and g.s. energies are included
- Consistent DWIA analysis in that the bound state wave function, spectroscopic factors and outgoing proton distorted wave are provided by the same DOM.

Outline

Uncertitude quantification

PHYSICAL REVIEW C **107**, 014602 (2023)

Uncertainty-quantified phenomenological optical potentials for single-nucleon scattering

C. D. Pruitt,* J. E. Escher, and R. Rahman†
Lawrence Livermore National Laboratory, Livermore, California 94550, USA

(Received 15 July 2022; accepted 29 November 2022; published 3 January 2023)

Optical-model potentials (OMPs) continue to play a key role in nuclear reaction calculations. However, the uncertainty of phenomenological OMPs in widespread use—inherent to any parametric model trained on data—has not been fully characterized, and its impact on downstream users of OMPs remains unclear. Here we assign well-calibrated uncertainties for two representative global OMPs, those of Koning-Delaroche and Chapel Hill '89, using Markov-chain Monte Carlo for parameter inference. By comparing the canonical versions of these OMPs against the experimental data originally used to constrain them, we show how a lack of outlier rejection and a systematic underestimation of experimental uncertainties contributes to bias of, and overconfidence in, best-fit parameter values. Our updated, uncertainty-quantified versions of these OMPs address these issues and yield complete covariance information for potential parameters. Scattering predictions generated

Uncertitude quantification

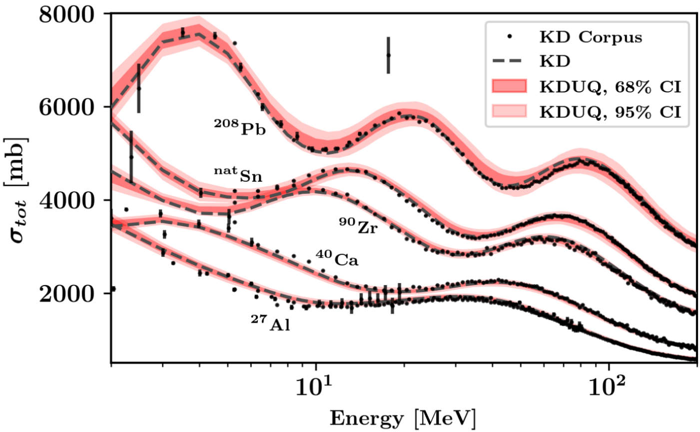

Outline

Microscopic approaches

Here we consider approaches starting from 2-body interaction. Many-body methods are then used to contruct the n-A interaction

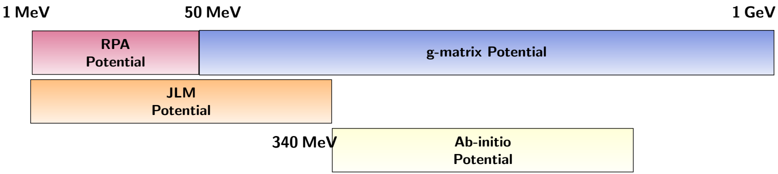

Optical potential depends on particle-hole & particle-particle correlations

- RPA potential accounts for particle-hole correlations (approximation valid below 40 MeV)
- g-matrix accounts for particle-particle correlations (approximation valid above 40 MeV)
- FRPA deals with both on the same footing

Outline

Ab-initio potential

Criteria:

- Based on bare NN interaction
- Consistency

Account for ph & pp correlations on the same footings

→ See Vittorio's talk

Diagram expansion for FRPA,

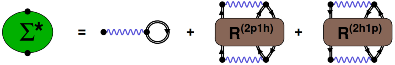

with the (2p-1h) propagator

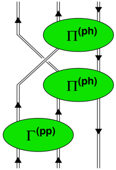

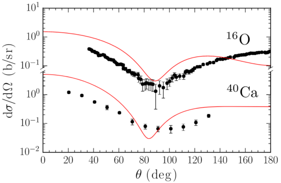

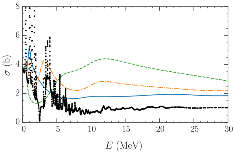

FIG. 4. Total elastic cross section for neutron elastic scattering on ^{16}O form SCGF ADC(3) at different incident neutron energies compared to the experiment in Ref. [51]. The dashed, dotted-dashed, and solid lines correspond to the sole static self-energy $\Sigma^{(\infty)}$, to retaining 50% of the $2p1h$ and $2h1p$ doorway configurations and to the complete Eq. (2), respectively.

A. Idini, C. Barbieri, P. Navrátil PRL 123, 092501

Self-energy obtained on harmonic oscillator basis then transformed in momentum space.

Account for ph & pp correlations on the same footings

$\rightarrow$ See Vittorio's talk

Diagram expansion for FRPA,

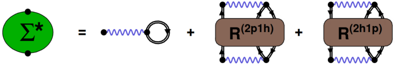

with the (2p-1h) propagator

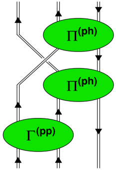

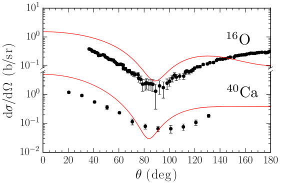

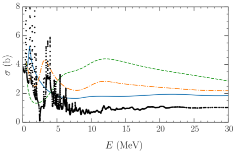

FIG. 4. Total elastic cross section for neutron elastic scattering on ^{16}O form SCGF ADC(3) at different incident neutron energies compared to the experiment in Ref. [51]. The dashed, dotted-dashed, and solid lines correspond to the sole static self-energy $\Sigma^{(\infty)}$, to retaining 50% of the $2p1h$ and $2h1p$ doorway configurations and to the complete Eq. (2), respectively.

A. Idini, C. Barbieri, P. Navrátil PRL 123, 092501

Self-energy obtained on harmonic oscillator basis then transformed in momentum space.

Lack of absorption. Need for higher-order calculations (3p-2h...)

Average in energy *vs.* Width(s)

- Averaging energy from Self-energy to optical potential
- Width to mimic continuum (escape width)
- Width to mimic higher orders (damping width)

Toward Gorkov-SCGF potential

PHYSICAL REVIEW C **89**, 024323 (2014)

Ab initio self-consistent Gorkov-Green's function calculations of semi-magic nuclei: Numerical implementation at second order with a two-nucleon interaction

V. Somà,[1,2,*] C. Barbieri,[3,†] and T. Duguet[4,5,‡]

[1]*Institut für Kernphysik, Technische Universität Darmstadt, 64289 Darmstadt, Germany*

[2]*ExtreMe Matter Institute EMMI, GSI Helmholtzzentrum für Schwerionenforschung GmbH, 64291 Darmstadt, Germany*

[3]*Department of Physics, University of Surrey, Guildford GU2 7XH, United Kingdom*

[4]*CEA-Saclay, IRFU/Service de Physique Nucléaire, 91191 Gif-sur-Yvette, France*

[5]*National Superconducting Cyclotron Laboratory and Department of Physics and Astronomy, Michigan State University, East Lansing, Michigan 48824, USA*

(Received 15 November 2013; published 28 February 2014)

Coupled cluster potential

Inversion of propagators using ab-initio wave functions

Dyson equation

$$G_1(1,1') = G_0(1,1') + \int d2d3 G_0(1,2) \underbrace{\Sigma(2,3)}_{\textbf{Self-energy}} G_1(3,1')$$

Rotureau, Danielewicz, Hagen, Jansen, Nunes arxiv: 1808.04535 and PRC 95, 024315 (2017)

Harmonic oscillators and coordinate space

Picture from J. Dobaczewski https://www.fuw.edu.pl/ dobaczew/thodri30w/node4.html

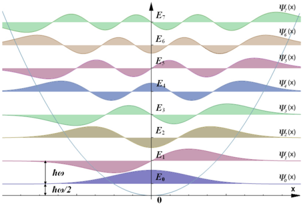

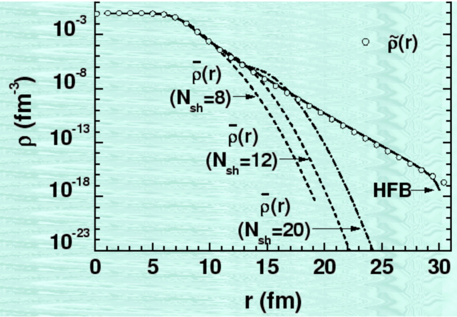

Picture from J. Dobaczewski https://www.fuw.edu.pl/ dobaczew/thodri30w/node4.html

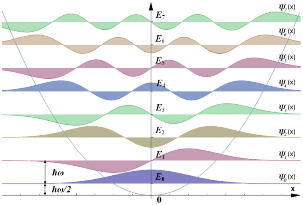

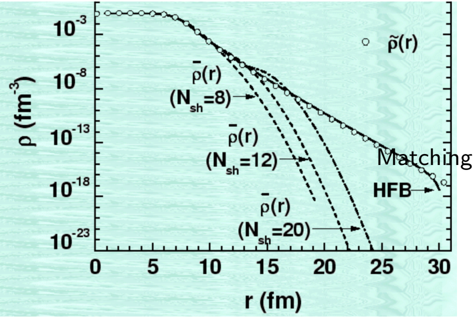

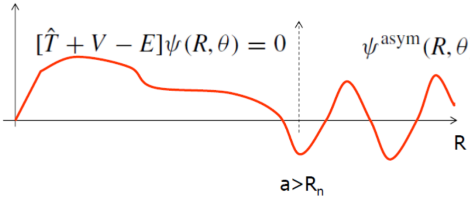

$$[\hat{T} + V - E]\psi(R,\theta) = 0$$

$$\psi^{\text{asym}}(R,\theta) = e^{ikz} + f(\theta)\frac{e^{ikR}}{R}$$

R_n : some large R where $V(R) \approx 0$ (potential dependent)

Outline

Bare $NN \to N + A$ connection

$$\underbrace{\boldsymbol{NN} \to \left\{ \begin{array}{c} \left(\frac{d\sigma}{d\Omega}\right)_{NN} \\ \downarrow\uparrow \\ \delta_L(E) \end{array} \right\}}_{\text{2-Body}} \rightleftharpoons v_{NN} \underbrace{\begin{array}{c} \nearrow \\ \searrow \end{array} \left. \begin{array}{c} \mathcal{G}_{NN} \\ \\ t_{NN} \end{array} \right\}}_{\text{Effective interaction}} \underbrace{\to \underbrace{U_{opt}(\mathbf{k}', \mathbf{k}; E)}_{\uparrow\ |\Psi_{g.s.}\rangle} \to \left\{ \begin{array}{c} |\psi\rangle \\ \frac{d\sigma}{d\Omega} \\ \sigma \end{array} \right.}_{\text{N+A}}$$

$$U(\mathbf{k}', \mathbf{k}; E) = \int d\mathbf{p} d\mathbf{p}' \quad \underbrace{\rho(\mathbf{p}', \mathbf{p})}_{\sim\sum \phi_\alpha(p')\phi^\dagger_\alpha(p)} \quad \underbrace{\langle \mathbf{k}' \, \mathbf{p}' \, | G(E, \rho) | \, \mathbf{k} \, \mathbf{p} \rangle}_{V_{NN}}$$

Use of LDA approximation

Une matrice-g fournie par Santiago avec le code

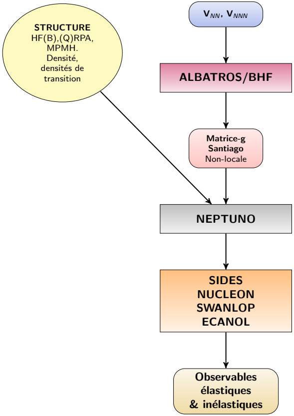

- Collaboration avec H. F. Arellano
- Maitrisée
- Nonlocalité conservée
- Fonctionne au-dessus de 40 MeV

Matrice-g de Santiago   40 MeV $< E <$ 1 GeV

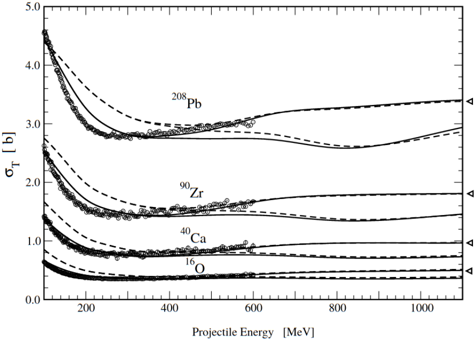

FIG. 3: Total cross section for neutron elastic scattering from ^{208}Pb, ^{90}Zr, ^{40}Ca and ^{16}O as functions of the projectile energy. The data [30] are represented with open circles. The solid and dashed curves represent full-folding results using the g- and t-matrix respectively. The curves corresponding to the full NNOMP are marked with a triangular label at their right end, whereas those results with the imaginary part of the NNOMP suppressed are unmarked.

Outline

A g-matrix corrected to fit low energy region

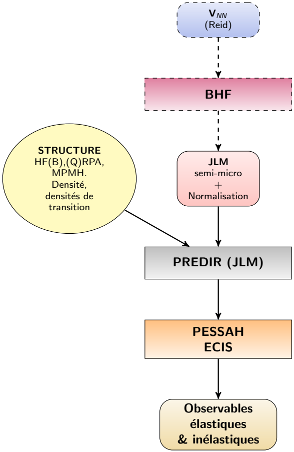

Principle:

- Jeukenne-Leujeune-Mahaux then Bauge then Dupuis
- BHF + ad-hoc parameters
- 2-effective interaction on Yukawas
- Local interaction
- Only direct terms are considered

  Resulting potential is local
- Allow for a consistent determination of both optical and transition potentials (inelastic scattering).

On going work:

- Add spin-orbit and tensor contributions

Available in Talys

Spherical optical potentials

$$\left(E - \hat{T} - \langle \psi_0 | \hat{V}_{\text{Eff.}} | \psi_0 \rangle \right) |w_0\rangle = 0$$

J.-P. Jeukenne, A. Lejeune, and C. Mahaux, Phys. Rev. C 16, 80, (1977)

JLM approach : semi-microscopic (phenomenology).
Brueckner-Hartree-Fock, Reid's hard core

→ Improved LDA : $V(\rho_{\mathrm{IS}}, \rho_{\mathrm{IV}}, E)$
→ Four E-dependent parameters : IS/IV components of Re/Im parts.
→ Fitted to reproduce elastic and charge exchange (Lane consistent).
→ Input : neutron and proton nuclear density profiles.

Global interaction (**Bauge et al. 2001**) : HFB densities,
→ E=1 keV – 200 MeV, recently 200 → 340 MeV.
→ A >~ 30 (limit of LDA)

Brueckner calculations : contains exchange.
Only direct part (local) kept for potential in finite nuclei.

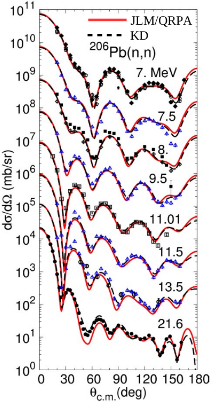

Slide from M. Dupuis

Whitehead-Lim-Hot (WLH) global optical potential

Outline

A microscopic potential for low incident energies based on effective interaction: Skyrme, Gogny

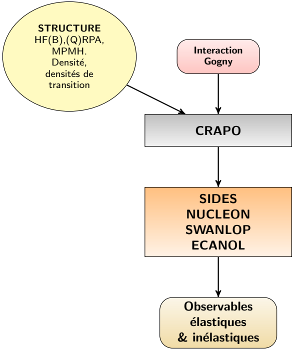

- Developped by N. Vinh Mau and A. Bouyssy
- $E < 40$ MeV

$$\begin{tikzcd} \rho \arrow[r, bend left, dashed, "\text{NN interaction}"] & V^{HF}(\rho) + \Delta V(\rho) \arrow[l, bend left, "\text{Schrödinger equation}"] \end{tikzcd}$$

SCRPA

Potential based on effective interaction

- Nuclear Structure Method developed by N. Vinh Mau
- Recent interest (Orsay, Hanoï, Japan, Milano, China, Bruyères, Russia)

Mean-Field and beyond from effective NN interaction $\longrightarrow$ Optical Potential

Goals

- Build an optical potential from an effective NN interaction
- Consistent use of the effective NN interaction
- Self-consistency

Tools

- Green's functions formalism
- Gogny D1S phenomenological effective interaction

Effective NN interaction: Pros and cons

Pros

- Phenomenological account of short range correlations
- Simple shape
- Energy independent
- Extended reach of EDF approaches

Cons

- Simple shape
- Validity out of the parametrization range
- Loss of the contact with more fundamental theories

Skyrme interaction Zero-range interaction

Gogny interaction

Finite-range interaction
(Brink and Boeker)

Extended reach of EDF approaches

Spherical Hartree-Fock (∼30 nuclei)

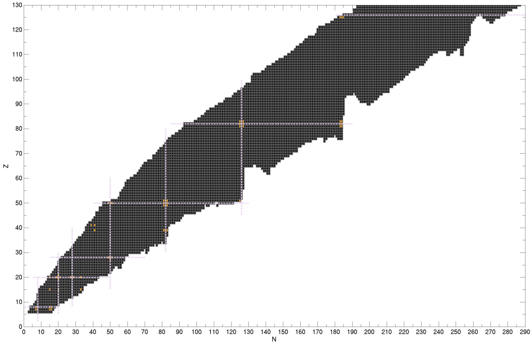

Calculations with Gogny D1S interaction (S. Hilaire and J.P. Ebran)

Extended reach of EDF approaches

Spherical Hartree-Fock-Bogoliubov (∼300 nuclei)

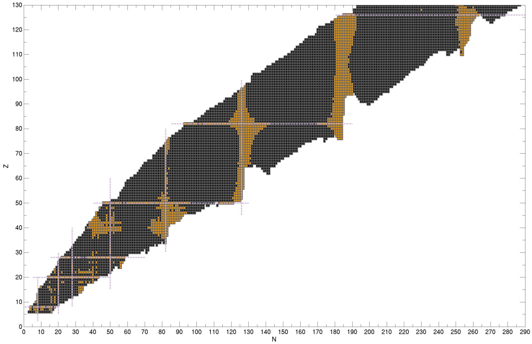

Calculations with Gogny D1S interaction (S. Hilaire and J.P. Ebran)

Axially-deformed Hartree-Fock-Bogoliubov ($\sim$6000 nuclei)

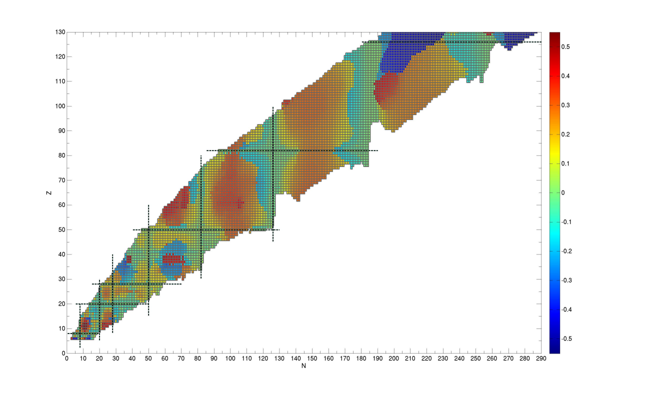

Calculations with Gogny D1S interaction (S. Hilaire and J.P. Ebran)

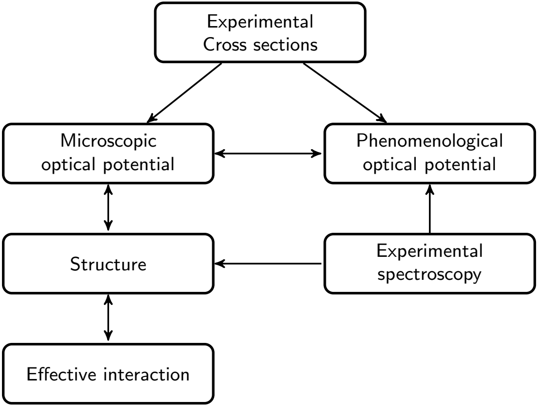
Experimental Cross sections
Microscopic optical potential
Phenomenological optical potential
Structure
Experimental spectroscopy
Effective interaction

Nuclear Structure Method (NSM)

$$V = V^{HF} + \Delta V^{RPA}$$

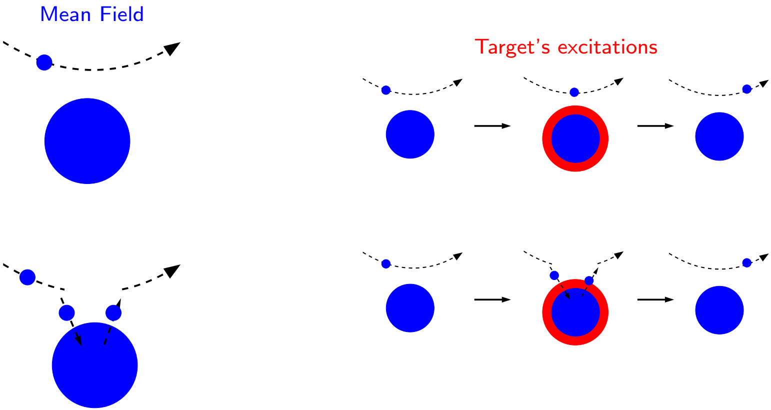

(N. Vinh Mau, Theory of nuclear structure (IAEA, Vienna) p. 931 (1970),

G. Blanchon, M. Dupuis, H.F. Arellano et N. Vinh Mau, PRC 91, 014612 (2015))

Bare Interaction

Optical potential

$$V = V^{HF} + V^{PP} + V^{RPA} - 2V^{(2)}$$

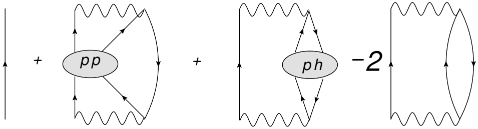

Optical potential

$$V = V^{HF} + V^{PP} + V^{RPA} - 2V^{(2)}$$

Bare Interaction

Effective Interaction

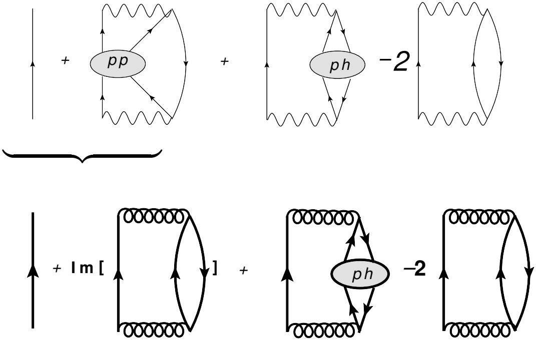

Optical potential

$$V = V^{HF} + V^{PP} + V^{RPA} - 2V^{(2)}$$

Bare Interaction

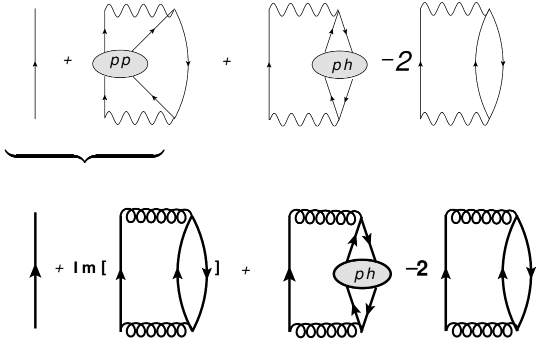

Gogny Interaction

Self-consistency

$$\begin{tikzcd}
\rho \arrow[r, bend left, "\text{NN interaction}"] & V^{HF}(\rho) \arrow[l, bend left, "\text{Schrödinger equation}"]
\end{tikzcd}$$

SCHF

$$\begin{tikzcd}
\rho \arrow[r, bend left, dashed, "\text{NN interaction}"] & V^{HF}(\rho) + \Delta V(\rho) \arrow[l, bend left, "\text{Schrödinger equation}"]
\end{tikzcd}$$

SCRPA

Elastic scattering n/p + ^{40}Ca

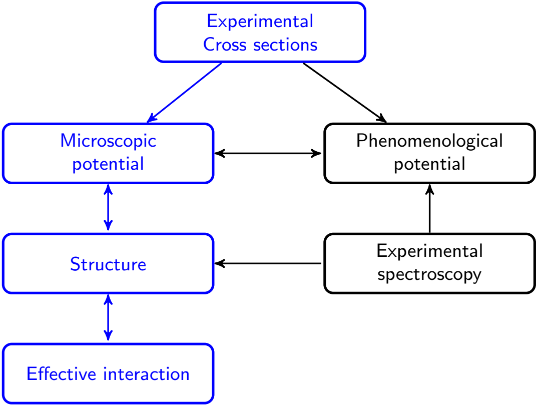

Schrödinger equation

$$\frac{p^2}{2m}\phi_\lambda(\mathbf{r},\varepsilon) + \int d\mathbf{r'}\,V^{HF}(\mathbf{r},\mathbf{r'};\varepsilon)\phi_\lambda(\mathbf{r'},\varepsilon) = E(\varepsilon)\phi_\lambda(\mathbf{r},\varepsilon)$$

HF potential

$$V^{HF}(\mathbf{r},\mathbf{r''};\varepsilon) = \delta(\mathbf{r},\mathbf{r''})\int d\mathbf{r'}\,v(\mathbf{r},\mathbf{r'})\rho(\mathbf{r'}) - v(\mathbf{r},\mathbf{r''})\rho(\mathbf{r},\mathbf{r''})$$

$$\begin{tikzcd}
\rho \arrow[r, bend left, "\text{NN interaction}"] & V^{HF}(\rho) \arrow[l, bend left, "\text{Schrödinger equation}"]
\end{tikzcd}$$

ph-RPA potential

$$\Delta V_{RPA} = \mathrm{Im}\left[V^{(2)}\right] + V^{RPA} - 2V^{(2)}$$

$$V^{RPA}(\mathbf{r},\mathbf{r}',E) = \lim_{\eta\to 0^+} \sum_{N\neq 0,ijkl}\sum_{\lambda}\!\!\!\!\!\!\int \chi_{ij}^{(N)}\chi_{kl}^{(N)}$$
$$\times \left(\frac{n_\lambda}{E-\epsilon_\lambda+E_N-i\Gamma(E_N)}+\frac{1-n_\lambda}{E-\epsilon_\lambda-E_N+i\Gamma(E_N)}\right) F_{ij\lambda}(\mathbf{r})F^*_{kl\lambda}(\mathbf{r}')$$

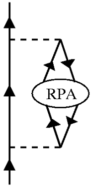

with

$$F_{ij\lambda}(\mathbf{r}) = \int d^3\mathbf{r}_1 \phi_i^*(\mathbf{r}_1)v(\mathbf{r},\mathbf{r}_1)[1-P]\phi_\lambda(\mathbf{r})\phi_j(\mathbf{r}_1)$$

- ϕ are HF wave functions.
- Bound as well as continuum states are taken into account for the intermediate state ϕ_λ.
- Target excitations are obtained from the spherical RPA/D1S code.

  Blaizot, et al., NPA 265, 315 (1976).

  Berger, et al., Comp. Phys. Com. 63, 365 (1991).

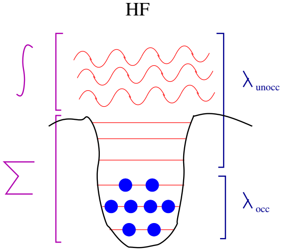

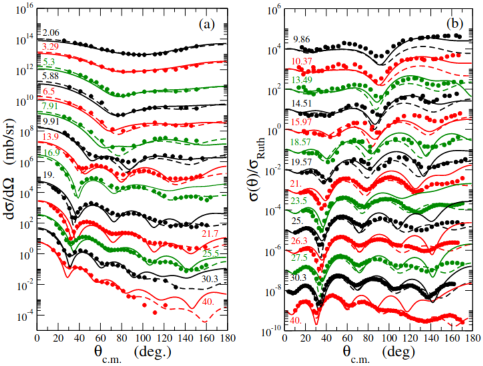

FIG. 1: Differential cross sections for neutron (a) and proton (b) scattering from ^{40}Ca. Comparison between data (symbols), $V^{HF} + \Delta V$ results (solid curves) and Koning-Delaroche potential results (dashed curves).

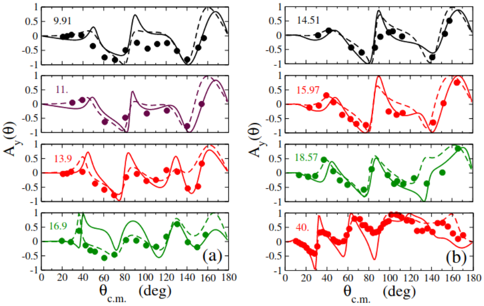

FIG. 2: Same as Fig. 1 for analyzing powers.

Outline

The optical potential as a possible connection between different levels of phenomenology

- Phenomenological optical potential
- Potentials based on phenomenological effective NN interaction (Gogny, Skyrme...)
- Ab-initio potentials based on phenomenological bare NN interaction

Optical potential

The optical potential as a possible connection between different levels of phenomenology

- Phenomenological optical potential
- Potentials based on phenomenological effective NN interaction (Gogny, Skyrme...)
- Ab-initio potentials based on phenomenological bare NN interaction

Possibility of fruitful exchanges between those communities

Probes and targets

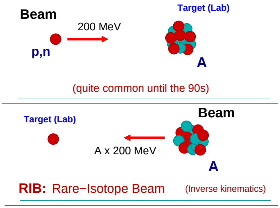

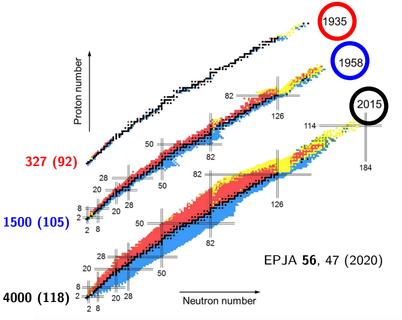

- **Motivations for studying optical potential:**
  - Key element for evaluations
  - Interpretation of experiments
  - Interesting by itself

- **Motivations for studying optical potential:**
  - Key element for evaluations
  - Interpretation of experiments
  - Interesting by itself

- **Different strategies:**
  - Microscopy: build the potential from NN interaction and many-body theory
  - Phenomenology: postulate a shape of potential and calibrate on experiment
  - Dialogue microscopy/phenomenology

Origin of nonlocality

- **Antisymmetrization**

$$V_{HF}(\mathbf{r},\mathbf{r'}) = \int d\mathbf{r}_1 \rho(\mathbf{r}_1) v(\mathbf{r},\mathbf{r}_1) - \rho(\mathbf{r},\mathbf{r'}) v(\mathbf{r},\mathbf{r'})$$

- **Antisymmetrization**

$$V_{HF}(\mathbf{r},\mathbf{r'}) = \int d\mathbf{r}_1 \rho(\mathbf{r}_1) v(\mathbf{r},\mathbf{r}_1) - \rho(\mathbf{r},\mathbf{r'}) v(\mathbf{r},\mathbf{r'})$$

- **Polarization**
Surface term...

$$\Delta U(\mathbf{r},\mathbf{r}';E) = \sum_i V_{0i}(\mathbf{r}) G_{ii}(\mathbf{r},\mathbf{r'};E) V_{i0}(\mathbf{r'}),$$

where G_{ii} is a propagator

$$V_{i0}(\mathbf{r}) = \beta_i r \frac{dU(r)}{dr} Y_\lambda^\mu(\widehat{\mathbf{r}}),$$

transition potential in the Bohr collective model.

A. Lev, W. P. Beres, and M. Divadeenam. PRC 9 :2416–2434, Jun 1974.

Woods and Saxon (phenomenological)

$$V(r) = -[V_0 + iW_0]f_{vol}(r) - iW_D f_{surf}(r) - (U_{so} + iW_{so}) f_{surf}(r)\, \boldsymbol{\ell} \cdot \boldsymbol{\sigma}$$

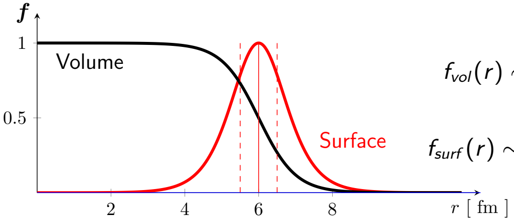

$$f_{vol}(r) \sim \frac{1}{1 + e^{(r - R_0)/a}}$$

$$f_{surf}(r) \sim \frac{4\, e^{(r - R_0)/a}}{[1 + e^{(r - R_0)/a}]^2}$$

Integro-différential scattering equation,

$$-\frac{\hbar^2}{2\mu}\Delta\psi(\mathbf{r}) + \int V_{NL}(\mathbf{r},\mathbf{r'})\psi(\mathbf{r'})\mathrm{d}\mathbf{r'} = E\psi(\mathbf{r}),$$

When potential is local

$$V_{NL}(\mathbf{r},\mathbf{r'}) = V_L(\mathbf{r})\delta(\mathbf{r},\mathbf{r'}).$$

Scattering equation reduces to **differential**,

$$-\frac{\hbar^2}{2\mu}\Delta\psi(\mathbf{r}) + V_L(\mathbf{r})\psi(\mathbf{r}) = E\psi(\mathbf{r}).$$

$\rightarrow$ **Need for numerical tools**

Outline

2.E

Nuclear Physics **32** (1962) 353—380; © *North-Holland Publishing Co., Amsterdam*

A NON-LOCAL POTENTIAL MODEL FOR THE SCATTERING OF NEUTRONS BY NUCLEI

F. PEREY and B. BUCK

Oak Ridge National Laboratory † *Oak Ridge, Tennessee*

Received 25 September 1961

Abstract: An energy independent non-local optical potential for the elastic scattering of neutrons from nuclei is proposed and the wave-equation solved numerically in its full integro-differential form. The non-local kernel is assumed separable into a potential form factor times a Gaussian non-locality. The potential form factor, of argument $\frac{1}{2}(\mathbf{r}+\mathbf{r}')$, is that of a real Saxon form plus an imaginary term having the shape of the derivative of a Saxon form. A real local spin-orbit potential of the usual Thomas form is included. The parameters of the potential obtained solely from the fitting of the differential cross sections for lead at 7 MeV and 14.5 MeV are used unchanged to calculate the elastic differential cross sections, total and reaction cross sections and polarizations on some elements ranging from Al to Pb at various energies from 0.4 MeV to 24 MeV. The S-wave strength functions and the effective scattering radius R' are also calculated with the same parameters. The parameters in the usual notations are: real potential $V = 71$ MeV, $r = 1.22$ fm, $a = 0.65$ fm; surface imaginary potential $W = 15$ MeV, $a = 0.47$ fm; non-locality $\beta = 0.85$ fm; spin-orbit potential, using the nucleon mass in the Thomas form, $U_{so} = 1300$ MeV. The energy independence of the

F. PEREY AND B. BUCK

linate representation, a non-local potential operating on a v
; the form

$$\boxed{V\Psi(\mathbf{r}) = \int V(\mathbf{r}, \mathbf{r}')\Psi(\mathbf{r}')\mathrm{d}\mathbf{r}'.}$$

faced with an integro-differential Schrödinger equation whic
by numerical integration and iteration.
al grounds it is necessary that the kernel function $V(\mathbf{r},$
, i.e.,

$$V(\mathbf{r}, \mathbf{r}') = V(\mathbf{r}', \mathbf{r}).$$

te the numerical calculations a separable form was chosen fo
rnel function:

$$\boxed{V(\mathbf{r}, \mathbf{r}') = U\left(\frac{\mathbf{r}+\mathbf{r}'}{2}\right) H\left(\frac{\mathbf{r}-\mathbf{r}'}{\beta}\right).}$$

nonlocality

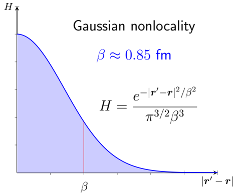

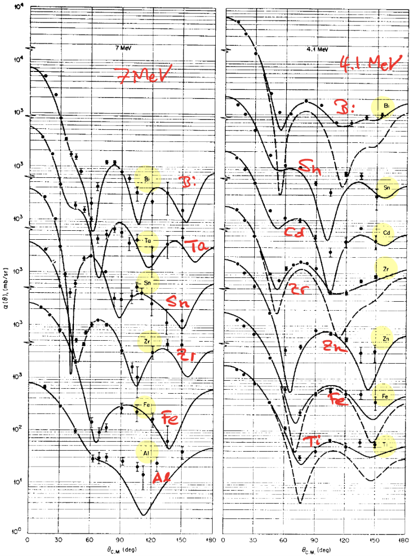

Fig. 2. Comparison of predictions of the energy independent non-local optical model with experimental elastic differential cross-sections of neutrons at 4.1 MeV and 7 MeV. The parameters are

Perey-Buck's assumptions:

- Separability
- Gaussian nonlocality
- Low incident energy $E < 24$ MeV
- Energy-independent
- Local spin-orbit

Perey-Buck's assumptions:

- Separability
- Gaussian nonlocality
- Low incident energy $E < 24$ MeV
- Energy-independent
- Local spin-orbit

$\rightarrow$ Shape used in most of nowadays phenomenology

Perey-Buck's assumptions:

- Separability
- Gaussian nonlocality
- Low incident energy $E < 24$ MeV
- Energy-independent
- Local spin-orbit

$\rightarrow$ Shape used in most of nowadays phenomenology

$\rightarrow$ Is it validated by microscopy? (at least by a given microscopic model)

Outline

Representations

$$\langle \text{post} | \hat{U} | \text{prior} \rangle$$

relative coordinates

$r', \ r, \ \hat{\boldsymbol{r}} \cdot \hat{\boldsymbol{r}}'$

$U(\boldsymbol{r}', \boldsymbol{r})$

$$\boldsymbol{R} = \frac{1}{2}(\boldsymbol{r}' + \boldsymbol{r})$$

'nonlocality' $\boldsymbol{s} = \boldsymbol{r}' - \boldsymbol{r}$

$s, \ R, \ \hat{\boldsymbol{R}} \cdot \hat{\boldsymbol{s}}$

relative momenta

$k', \ k, \ \hat{\boldsymbol{k}} \cdot \hat{\boldsymbol{k}}'$

$\tilde{U}(\boldsymbol{k}', \boldsymbol{k})$

$\boldsymbol{q} = \boldsymbol{k}' - \boldsymbol{k}$ momentum transfer

$$\boldsymbol{K} = \frac{1}{2}(\boldsymbol{k}' + \boldsymbol{k})$$

$K, \ q, \ \hat{\boldsymbol{K}} \cdot \hat{\boldsymbol{q}}$

Bare $NN \rightarrow N + A$ connection

$$\underbrace{\boldsymbol{N}N \rightarrow \left\{ \begin{array}{c} \left(\frac{d\sigma}{d\Omega}\right)_{NN} \\ \downarrow\uparrow \\ \delta_L(E) \end{array} \right\}}_{\text{2-Body}} \rightleftharpoons v_{NN} \underbrace{\begin{array}{c} \nearrow \\ \searrow \end{array} \left. \begin{array}{c} \mathcal{G}_{NN} \\ \\ t_{NN} \end{array} \right\}}_{\text{Effective interaction}} \rightarrow \underbrace{\underbrace{U_{opt}(\mathbf{k}', \mathbf{k}; E)}_{\uparrow\ |\Psi_{g.s.}\rangle} \rightarrow \left\{ \begin{array}{c} |\psi\rangle \\ \frac{d\sigma}{d\Omega} \\ \sigma \end{array} \right.}_{\text{N+A}}$$

$$U(\mathbf{k}', \mathbf{k}; E) = \int d\mathbf{p} d\mathbf{p}' \quad \underbrace{\rho(\mathbf{p}', \mathbf{p})}_{\sim\sum \phi_\alpha(p')\phi^\dagger_\alpha(p)} \quad \underbrace{\langle \mathbf{k}'\, \mathbf{p}' \,|G(E,\rho)|\, \mathbf{k}\, \mathbf{p} \rangle}_{V_{NN}}$$

Check that microscopy works...

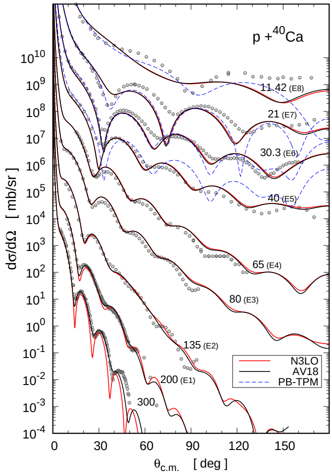

- Tian-Pang-Ma
- N3LO / Density from Gogny HFB
- AV18 / Density from Gogny HFB

$\tilde{U}$ in the K-q plane

Weak angular dependence ($w = \hat{K}\cdot\hat{q}$)

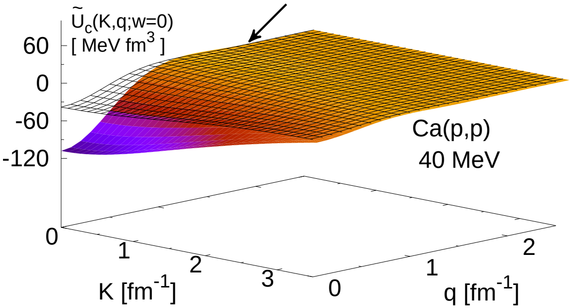

$$\tilde{U}(K,q) = \frac{\tilde{U}(K,q)}{\tilde{U}(K,0)} \times \frac{\tilde{U}(K,0)}{\tilde{U}(0,0)} \times \tilde{U}(0,0) \equiv \tilde{V}(K,q) \times \tilde{H}(K) \times W$$

Nonlocality

Strength

Weak K-dependence!

$\tilde{V}_c(K,q)=\tilde{U}(K,q)/\tilde{U}(K,0)\sim \tilde{v}(q)$ in the range 10–300 MeV

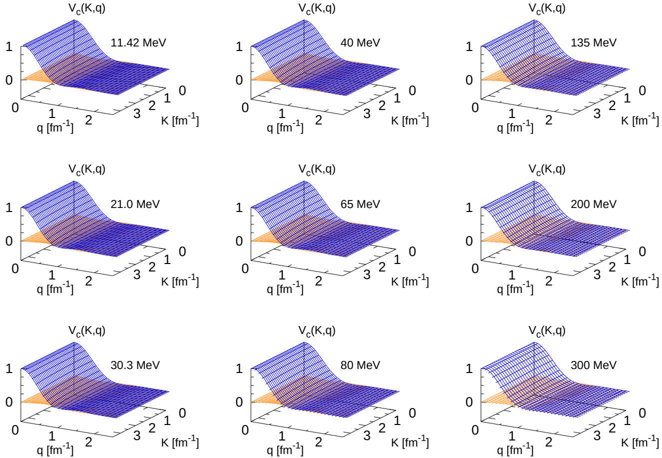

JvH factorization

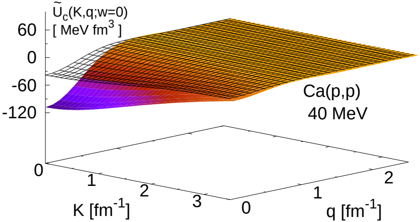

$$\tilde{U}(K,q) = W\,\tilde{v}(q)\,\tilde{H}(K)$$

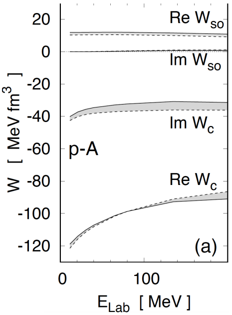

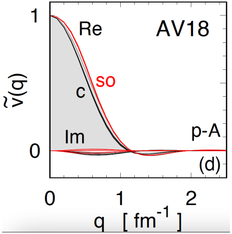

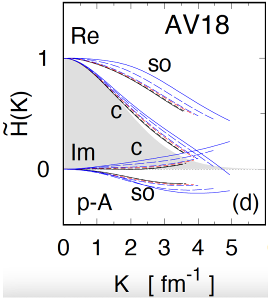

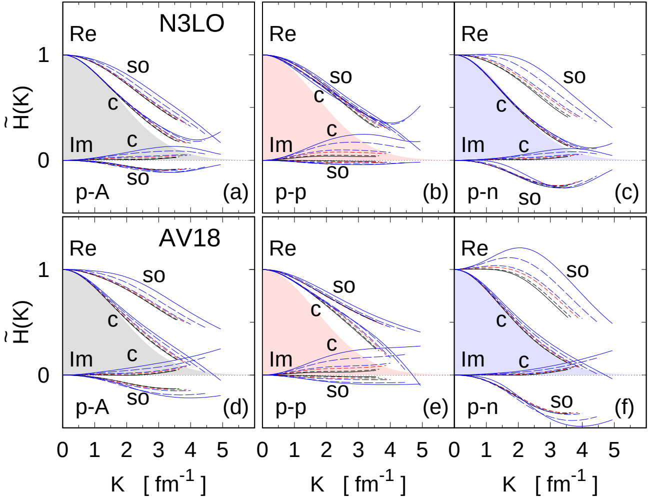

$$H_{PB}(s) = \frac{1}{\pi^{3/2}\beta^3} e^{-s^2/\beta^2}$$

$$\tilde{H}_{PB}(K) = e^{-\beta^2 K^2/4}$$

		N3LO			AV18		
	Energy (MeV)	β_{pA} (fm)	β_{pp} (fm)	β_{pn} (fm)	β_{pA} (fm)	β_{pp} (fm)	β_{pn} (fm)
Central	11.42	0.89	0.72	0.94	0.89	0.73	0.95
	21.0	0.88	0.72	0.94	0.89	0.72	0.94
	30.3	0.88	0.71	0.93	0.88	0.71	0.94
	40.0	0.88	0.71	0.93	0.88	0.71	0.93
	61.4	0.87	0.72	0.93	0.86	0.70	0.92
	80.0	0.87	0.72	0.93	0.86	0.71	0.92
	135.0	0.87	0.75	0.92	0.83	0.71	0.89
	200.0	0.86	0.78	0.90	0.80	0.72	0.85
Spin-orbit	11.42	0.57	0.61	0.51	0.47	0.58	0.03
	21.0	0.58	0.61	0.50	0.46	0.59	—
	30.3	0.58	0.62	0.49	0.48	0.59	—
	40.0	0.58	0.63	0.48	0.48	0.60	—
	61.4	0.57	0.63	0.43	0.46	0.60	—
	80.0	0.55	0.62	0.37	0.37	0.59	—
	135.0	0.48	0.59	0.13	0.32	0.56	—
	200.0	0.44	0.56	—	0.22	0.51	—

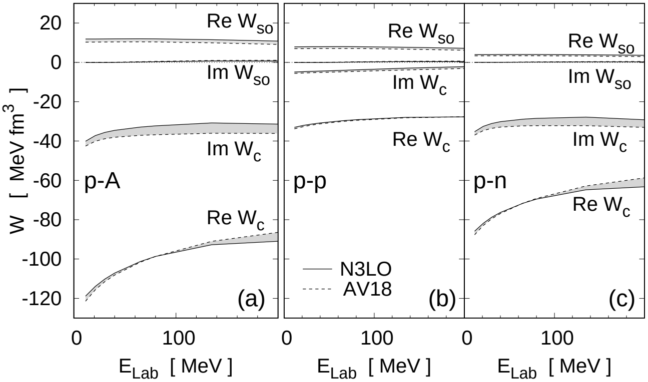

Volume integral

$$W = \frac{J}{(2\pi)^3}$$

Microscopic potential *vs.* JvH

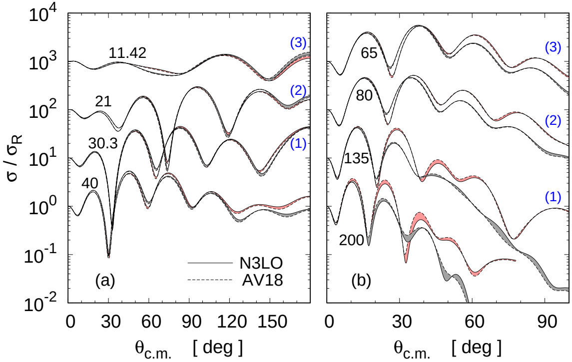

Nonlocalities for n+A & p+A

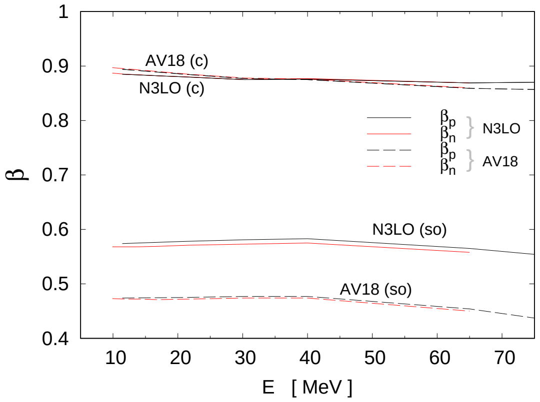

Concluding remarks

- To the lower order in the angular expansion $\widehat{\mathbf{q},\mathbf{K}}$ the microscopic potential leads to *JvH* separable structure of the central and the spin-orbit.
- Using our microscopic model, separability is validated for about $E < 30$MeV
- *JvH* validates Gaussian nonlocality.
- For $E < 65\ MeV$, the range of the nonlocality β is 0.86-0.89 fm for the central part and 0.46-0.58 for spin-orbit part.
- *JvH* offers a new link between theory and phenomenology. It will be interesting to explore higher orders.

Outline

- TALYS, CONRAD, EMPIRE

Phaseshift determination

Integro-differential Schrödinger equation

$$-\frac{\hbar^2}{2m}\left[\frac{d^2}{dr^2}-\frac{l(l+1)}{r^2}\right]u_{ljm}(r)+\int dr'\, r\nu_{ljm}(r,r')r'\,u_{jlm}(r') = E\ u_{ljm}(r)$$

Equations can be expressed on a radial mesh with h the step. The potential is negligible at $R_{max} = h \times N$.

$$\begin{aligned} u(r) &\longrightarrow u_i \\ \frac{d^2}{dr^2}u(r) &\longrightarrow \frac{u_{i+1}-2u_i+u_{i-1}}{h^2} \\ \nu(r,r') &\longrightarrow \nu_{ij} \end{aligned}$$

Schrödinger equation reads

$$\left[\begin{pmatrix} -2 & 1 & & & \\ 1 & -2 & 1 & & \\ & \ddots & \ddots & \ddots & \\ & & 1 & -2 & 1 \\ & & & 1 & -2 \end{pmatrix} + \begin{pmatrix} M_{1,1} & \cdots & & \\ \vdots & \ddots & & \\ & & \ddots & \vdots \\ & & \cdots & M_{N,N} \end{pmatrix}\right]\begin{pmatrix} u_1 \\ \vdots \\ u_N \end{pmatrix} = \begin{pmatrix} 0 \\ \vdots \\ 0 \\ -1 \end{pmatrix}$$

Conditions at the limits: $u_0 = 0,\ u_{N+1} = 1,\ M_{i,N+1} = 0$

Phaseshift determination

$$\sum_k \mathcal{M}_{i,k} u_k = \begin{pmatrix} 0 \\ \vdots \\ \\ 0 \\ -1 \end{pmatrix}$$

Solution merges from matrix inversion

$$u_i = -\left(\mathcal{M}^{-1}\right)_{i,N}$$

Solution can further be re-injected into Schrödinger equation with better precision and iterated until the needed precision is obtained.

Phaseshift determination

Connection to asymptotic solutions

$$u_{lj}(r) \underset{r\to+\infty}{=} C[\cos(\delta_{lj})j_l(kr) - \sin(\delta_{lj})n_l(kr)]$$

$$\text{avec} \qquad k^2 = -(2m/\hbar^2) \times E$$

with j_l, n_l Bessel and Neumann spherical functions.

Normalisation by a Dirac in energy

$$C = \sqrt{\frac{1}{\pi}\frac{2m}{\hbar^2 k}}$$

Phaseshift is obtained from

$$\frac{u_N'}{u_N} = \frac{\cos(\delta_{lj})j_l'(kR_{max}) - \sin(\delta_{lj})n_l'(kR_{max})}{\cos(\delta_{lj})j_l(kR_{max}) - \sin(\delta_{lj})n_l(kR_{max})}$$

Phaseshift determination

Connection to asymptotic solutions

$$u_{lj}(r) \underset{r \to +\infty}{=} C[\cos(\delta_{lj}) j_l(kr) - \sin(\delta_{lj}) n_l(kr)]$$

$$\text{avec} \qquad k^2 = -(2m/\hbar^2) \times E$$

with j_l, n_l Bessel and Neumann spherical functions.

Normalisation by a Dirac in energy

$$C = \sqrt{\frac{1}{\pi} \frac{2m}{\hbar^2 k}}$$

Phase shift

$$\tan(\delta_{lj}) = \frac{u_N j_l'(kR_{max}) - u_N' j_l(kR_{max})}{u_N n_l'(kR_{max}) - u_N' n_l(kR_{max})}$$

La diffusion de nucléon à PN

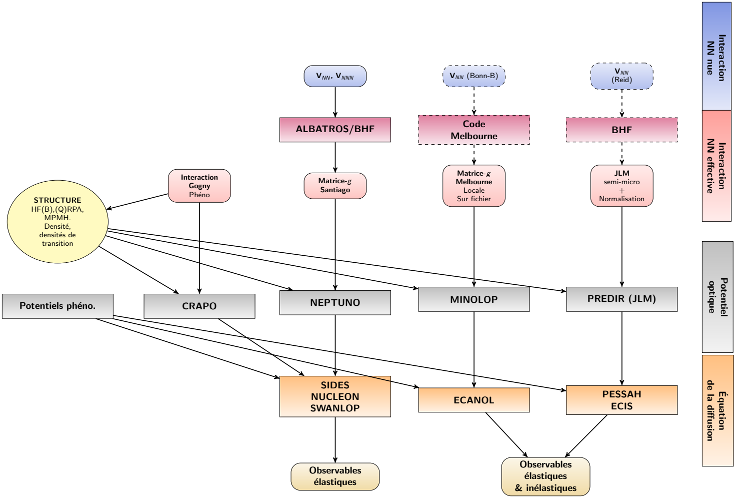

Faire évoluer les outils numériques pour gagner en efficacité et pour ouvrir de nouvelles perspectives.

... et peu à peu s'émanciper des codes de Jacques Raynal: DWBA et ECIS

- Diffusion non-locale: DWBA $\rightarrow$ NUCLEON,SIDES,SWANLOP
  - *SIDES: Schrödinger Integro-Differential Equation Solver*
    Méthode de Numérov modifiée de J. Raynal
    G. Blanchon, M. Dupuis, H. F. Arellano, R. N. Bernard, B. Morillon, CPC 254 (2020) 107340
  - *SWANLOP: Scattering WAve NonLOcal Potential*
    Résolution de l'équation de Lippmann-Schwinger
    H. F. Arellano, G. Blanchon, CPC 259 (2021) 107543
  - *NUCLEON*
    Résolution sur base de polynômes de Tchebyshev *(B. Morillon)*
- Voies couplées locales: ECIS $\rightarrow$ PESSAH
  Un code plus rapide et parallélisé *(P. Romain)*
- Voies couplées non-locales: ECANOL
  A. Nasri, M. Dupuis, G. Blanchon, H. F. Arellano and P. Tamagno, EPJA (2021) 57: 279

Potentiels proposés

- Koning-Delaroche global local potential *(de 1 keV à 200 MeV)*

  A. J. Koning and J.-P. Delaroche NPA 713(3-4) 231 - 310, 2003.

- Morillon-Romain global dispersive local potential *(de 1 keV à 200 MeV)*

  B. Morillon and P. Romain. PRC, 70 014601 (2004) and PRC, 76(4) 044601 (2007).

- Morillon global dispersive nonlocal potential *(Talk)*

- Perey-Buck global nonlocal potential *(below 30 MeV)*

  F. Perey and B. Buck. Nucl. Phys., 32 353 – 380, 1962.

- Tian-Pang-Ma global nonlocal potential *(below 30 MeV)*

  Y. Tian, D.-Y. Pang, and Z.-Y. Ma. IJMP E, 24(01) 1550006, 2015.

- Mahzoon nonlocal dispersive potential

  M. H. Mahzoon, R. J. Charity, W. H. Dickhoff, H. Dussan, and S. J. Waldecker. PRL 112 162503, 2014.

+ Potentiels sur un mesh radial ou en moment

NUCLEON, SIDES, SWANLOP validés avec le code DWBA

Résolution de l'équation de Schrödinger intégro-differentielle

$$-\frac{\hbar^2}{2\mu}\left[\frac{d^2}{dr^2}-\frac{l(l+1)}{r^2}\right]f_{lj}(k,r)+r\int_0^\infty \nu_{lj}(r,r';E)f_{lj}(k,r')r'\,\mathrm{d}r' = Ef_{lj}(k,r),$$

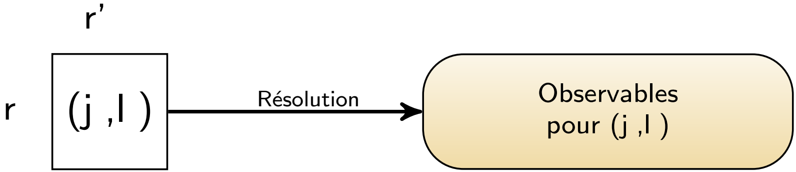

Non-local, Voies non-couplées

NUCLEON, SIDES, SWANLOP validés avec le code DWBA

Résolution de l'équation de Schrödinger intégro-differentielle

$$-\frac{\hbar^2}{2\mu}\left[\frac{d^2}{dr^2}-\frac{l(l+1)}{r^2}\right]f_{lj}(k,r)+r\int_0^\infty \nu_{lj}(r,r';E)f_{lj}(k,r')r'\,\mathrm{d}r' = Ef_{lj}(k,r),$$

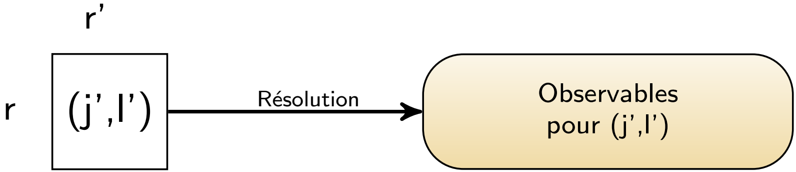

Code ECANOL (Thèse d'Amine Nasri)

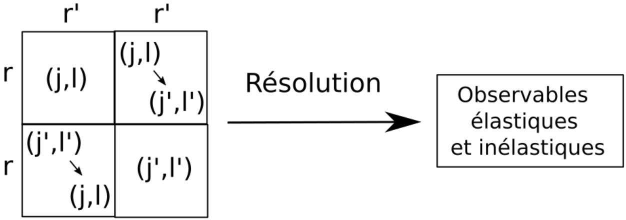

Validation de ECANOL avec le code DWBA

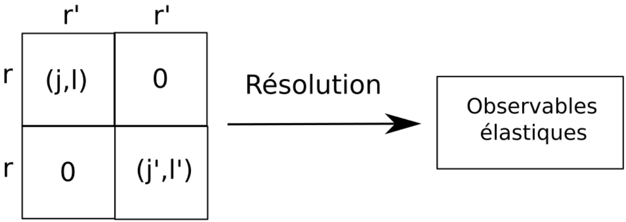

Validation de ECANOL avec le code ECIS

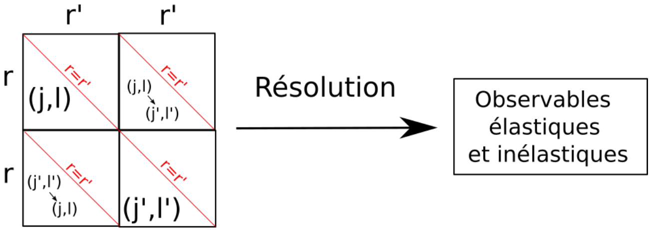

SCATTERING OFF TARGET WITH PAIRING

Spherical Hartree-Fock (∼30 nuclei)

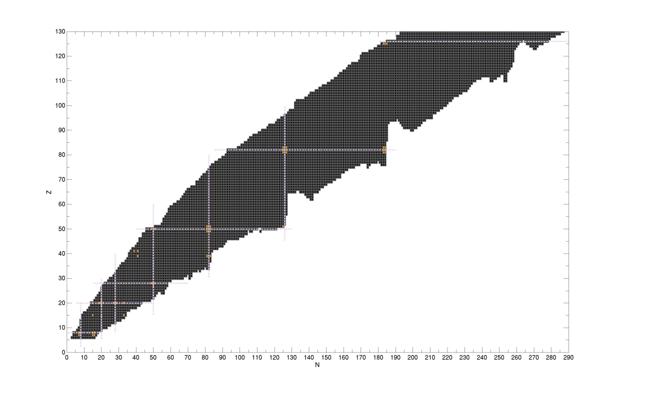

Calculations with Gogny D1S interaction (S. Hilaire and J.P. Ebran)

Spherical Hartree-Fock-Bogoliubov (∼300 nuclei)

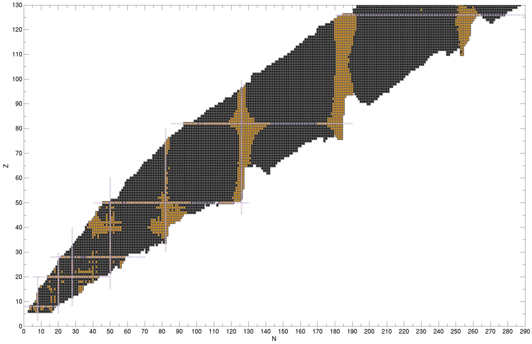

Calculations with Gogny D1S interaction (S. Hilaire and J.P. Ebran)

Axially-deformed Hartree-Fock-Bogoliubov (∼6000 nuclei)

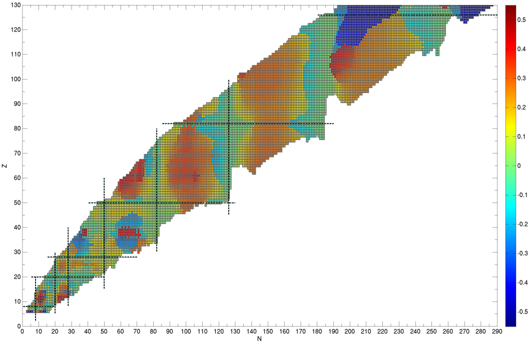

Calculations with Gogny D1S interaction (S. Hilaire and J.P. Ebran)

Quasiparticle scattering

HFB equations in coordinate space

$$\int d^3\mathbf{r'} \sum_{\sigma'} \begin{pmatrix} h(\mathbf{r}\sigma, \mathbf{r'}\sigma') & \Delta(\mathbf{r}\sigma, \mathbf{r'}\sigma') \\ \Delta(\mathbf{r}\sigma, \mathbf{r'}\sigma') & -h(\mathbf{r}\sigma, \mathbf{r'}\sigma') \end{pmatrix} \begin{pmatrix} \phi_1(E, \mathbf{r'}\sigma') \\ \phi_2(E, \mathbf{r'}\sigma') \end{pmatrix} = \begin{pmatrix} E+\lambda & 0 \\ 0 & E-\lambda \end{pmatrix} \begin{pmatrix} \phi_1(E, \mathbf{r}\sigma) \\ \phi_2(E, \mathbf{r}\sigma) \end{pmatrix}$$

- $h(\mathbf{r}\sigma, \mathbf{r'}\sigma') \equiv$ Kinetic term and mean-field
- $\Delta(\mathbf{r}\sigma, \mathbf{r'}\sigma') \equiv$ Pairing field

Multipole expansion in terms of (j, l)

$$\begin{cases} \phi_1(E, \mathbf{r}\sigma) = \frac{u_{lj}(E,r)}{r} \mathcal{Y}^m_{jl1/2}(\hat{\mathbf{r}}\sigma) \\ \phi_2(E, \mathbf{r}\sigma) = \frac{v_{lj}(E,r)}{r} \mathcal{Y}^m_{jl1/2}(\hat{\mathbf{r}}\sigma) \end{cases}$$

HFB fields and the chemical potential λ are extracted from an HFB/D1S code.

(Dechargé, Gogny PRC 21, 1568 (1980))

For a given (j, l), we have

$$\begin{pmatrix} h_{1,1}-(E+\lambda) & \dots & h_{1,N} & \Delta_{1,1} & \dots & \Delta_{1,N} \\ \vdots & \ddots & \vdots & \vdots & \ddots & \vdots \\ h_{N,1} & \dots & h_{N,N}-(E+\lambda) & \Delta_{N,1} & \dots & \Delta_{N,N} \\ \Delta_{1,1} & \dots & \Delta_{1,N} & -h_{1,1}-(E-\lambda) & \dots & -h_{1,N} \\ \vdots & \ddots & \vdots & \vdots & \ddots & \vdots \\ \Delta_{N,1} & \dots & \Delta_{N,N} & -h_{N,1} & \dots & -h_{N,N}-(E-\lambda) \end{pmatrix} \begin{pmatrix} u_1 \\ \vdots \\ u_N \\ v_1 \\ \vdots \\ v_N \end{pmatrix} = \begin{pmatrix} 0 \\ \vdots \\ -Y_0 \\ 0 \\ \vdots \\ Y_1 \end{pmatrix}$$

- Conditions at the limits:

$$\begin{cases} u_0 = v_0 = 0 \\ u_{N+1} = Y_0 \\ v_{N+1} = Y_1 \end{cases}$$

- Inversion of the matrix $(2N \times 2N)$ $\mathcal{M}$ gives the solutions

$$\begin{aligned} u_i &= -Y_0 \left(\mathcal{M}^{-1}\right)_{i,N} + Y_1 \left(\mathcal{M}^{-1}\right)_{i,2N} \\ v_i &= -Y_0 \left(\mathcal{M}^{-1}\right)_{i+N,N} + Y_1 \left(\mathcal{M}^{-1}\right)_{i+N,2N} \end{aligned}$$

- Mean field and pairing fields are zero at $R_{max} = N \times h$
- Connecting to asymptotic solutions for $(E + \lambda) > 0$

$$
\begin{aligned}
u_{lj}(r) &\underset{r \to +\infty}{=} C[\cos(\delta_{lj}) j_l(\alpha r) - \sin(\delta_{lj}) n_l(\alpha r)] \\
v_{lj}(r) &\underset{r \to +\infty}{=} D h_l(\beta r)
\end{aligned}
$$

with h_l the spherical Hankel function, $\alpha^2 = -(2m/\hbar^2)(\lambda + E)$, $\beta^2 = (2m/\hbar^2)(\lambda - E)$.

- u is normalized by a Dirac in energy $\rightarrow C$
- Y_0, Y_1, D et δ_{lj} are determined ensuring the continuity of u, v, u' et v' at R_{max}

Outline

A message from the 50's

Lecture from Claude Bloch 1955:
...in order to obtain a theory of nuclear reactions usable for the interpretation of experiments, it is advisable to avoid introducing a too detailed description of the nuclei, which could only be done at the cost of very rough approximations. In this way, one gives up the idea of relating all the experimental results to the laws governing elementary phenomena. What we will try to do is to define a minimum number of parameters sufficient to describe the observational results. The interest of such a theory is to reduce a large number of experimental results to a smaller number of parameters. The disadvantage of the method is that the parameters introduced in this way do not have a fundamental meaning. It will be up to a more sophisticated theory to relate them to the interaction laws of elementary particles.

A message from the 50's

Lecture from Claude Bloch 1955:
...in order to obtain a theory of nuclear reactions usable for the interpretation of experiments, it is advisable to avoid introducing a too detailed description of the nuclei, which could only be done at the cost of very rough approximations. In this way, one gives up the idea of relating all the experimental results to the laws governing elementary phenomena. What we will try to do is to define a minimum number of parameters sufficient to describe the observational results. The interest of such a theory is to reduce a large number of experimental results to a smaller number of parameters. The disadvantage of the method is that the parameters introduced in this way do not have a fundamental meaning. It will be up to a more sophisticated theory to relate them to the interaction laws of elementary particles.

A message from the 50's

Lecture from Claude Bloch 1955:

...in order to obtain a theory of nuclear reactions usable for the interpretation of experiments, it is advisable to avoid introducing a too detailed description of the nuclei, which could only be done at the cost of very rough approximations. In this way, one gives up the idea of relating all the experimental results to the laws governing elementary phenomena. What we will try to do is to define a minimum number of parameters sufficient to describe the observational results. The interest of such a theory is to reduce a large number of experimental results to a smaller number of parameters. The disadvantage of the method is that the parameters introduced in this way do not have a fundamental meaning. It will be up to a more sophisticated theory to relate them to the interaction laws of elementary particles.

A message from the 50's

Lecture from Claude Bloch 1955:
...*in order to obtain a theory of nuclear reactions usable for the interpretation of experiments, it is advisable to avoid introducing a too detailed description of the nuclei, which could only be done at the cost of very rough approximations. In this way, one gives up the idea of relating all the experimental results to the laws governing elementary phenomena. What we will try to do is to define a minimum number of parameters sufficient to describe the observational results. The interest of such a theory is to reduce a large number of experimental results to a smaller number of parameters. The disadvantage of the method is that the parameters introduced in this way do not have a fundamental meaning. It will be up to a more sophisticated theory to relate them to the interaction laws of elementary particles.*

- Systematics are made possible with comping power

- **Sujets non abordés dans cette présentation:**
  - Diffusion de particules composites
  - Potentiels déformés non-locaux phénoménologiques
  - Justification microscopique du potentiel Perey-Buck
  - Les approches mathématiques autour des potentiels optiques *(P. Chau et B. Ducomet)*
  - Les potentiels ab-inito au CEA

FURTHER READINGS

- *Quelques applications du formalisme des fonctions de Green à l'étude des noyaux*, N. Vinh Mau
- *Quantum Theory of Many-Particle Systems*, Fetter and Walecka.
- *A Guide to Feynman Diagrams in the Many-Body Problem*, Mattuck.
- *Quantum Statistical Mechanics: Green's Function Methods in Equilibrium and Non-Equilibrium Problems*, Kadanoff.
- *The nuclear many-body problem*, Ring and Schuck.
- *Optical potentials for the rare-isotope beam era*, Hebborn *et al*.